



National Library
of Canada

Bibliothèque nationale
du Canada

Canadian Theses Service

Service des thèses canadiennes

Ottawa, Canada
K1A 0N4

NOTICE

The quality of this microform is heavily dependent upon the quality of the original thesis submitted for microfilming. Every effort has been made to ensure the highest quality of reproduction possible.

If pages are missing, contact the university which granted the degree.

Some pages may have indistinct print especially if the original pages were typed with a poor typewriter ribbon or if the university sent us an inferior photocopy.

Reproduction in full or in part of this microform is governed by the Canadian Copyright Act, R.S.C. 1970, c. C-30, and subsequent amendments.

AVIS

La qualité de cette microforme dépend grandement de la qualité de la thèse soumise au microfilmage. Nous avons tout fait pour assurer une qualité supérieure de reproduction.

S'il manque des pages, veuillez communiquer avec l'université qui a conféré le grade.

La qualité d'impression de certaines pages peut laisser à désirer, surtout si les pages originales ont été dactylographiées à l'aide d'un ruban usé ou si l'université nous a fait parvenir une photocopie de qualité inférieure.

La reproduction, même partielle, de cette microforme est soumise à la Loi canadienne sur le droit d'auteur, SRC 1970, c. C-30, et ses amendements subséquents.

Iron Mediated Allylic Alkylation Reactions

By

Michel M. J. Bisnaire

A thesis submitted to the School of Graduate Studies in
partial fulfillment of the requirements for the degree of

Master of Science
in Chemistry

Department of Chemistry
University of Ottawa
Ottawa, Canada

Jean-Louis Roustan
Associate Professor of Chemistry
Research Supervisor

Michel M. J. Bisnaire
M.Sc. Candidate



Michel M.J. Bisnaire, Ottawa, Canada, 1990



National Library
of Canada

Bibliothèque nationale
du Canada

Canadian Theses Service Service des thèses canadiennes

Ottawa, Canada
K1A 0N4

The author has granted an irrevocable non-exclusive licence allowing the National Library of Canada to reproduce, loan, distribute or sell copies of his/her thesis by any means and in any form or format, making this thesis available to interested persons.

The author retains ownership of the copyright in his/her thesis. Neither the thesis nor substantial extracts from it may be printed or otherwise reproduced without his/her permission.

L'auteur a accordé une licence irrévocable et non exclusive permettant à la Bibliothèque nationale du Canada de reproduire, prêter, distribuer ou vendre des copies de sa thèse de quelque manière et sous quelque forme que ce soit pour mettre des exemplaires de cette thèse à la disposition des personnes intéressées.

L'auteur conserve la propriété du droit d'auteur qui protège sa thèse. Ni la thèse ni des extraits substantiels de celle-ci ne doivent être imprimés ou autrement reproduits sans son autorisation.

ISBN 0-315-60090-X

Canada



UNIVERSITÉ D'OTTAWA
UNIVERSITY OF OTTAWA

Abstract

In this work it will be shown that $\text{Fe}(\text{CO})_2(\text{NO})_2$ mediated allylic alkylation reactions proceed via an intermediate which is neither an η^3 -allyliron complex nor an η^2 -allyliron complex. Rather, $(\text{Fe}(\text{CO})(\text{NO})_2\text{DMM})^- \text{Na}^+$ has been identified as the catalytic intermediate. This provides the first evidence of an interaction between the nucleophile and the metallic center in reactions involving iron nitrosyl complexes. The study of the $\text{Fe}(\text{CO})_3(\text{NO})^- \text{Na}^+$, geranyl acetate, and NaDMM system was studied in order to elucidate the catalytically active species. Although it was determined that $\text{Fe}(\text{CO})_3(\text{NO})^- \text{Na}^+$ served as the precursor of a catalytic species X, the nature of X remains unknown.

List of Abbreviations

atm atmosphere
bpy 2,2'-bipyridyl
Bu₄N⁺ tetrabutyl ammonium cation
DEM diethylmalonate
DMF dimethyl formamide
DMM dimethylmalonate
dppe 1,2-bis (diphenylphosphino) ethane
Et ethyl
GC gas chromatogram
h hours
IR infra red
M⁺ molecular ion peak
Me methyl
mesi mesitylene
min minutes
MS mass spectrum
NaDMM sodium dimethylmalonate
NMR nuclear magnetic resonance
Nu nucleophile
OAc acetate Ph phenyl
RT retentiontime
TLC thin layer chromatography
TMS tetramethylsilane

Contents

List of Figures	8
List of Tables	10
1 Introduction	11
1.1 Transition Metal Mediated Catalytic Allylic Alkylation	11
1.2 Palladium Mediated Allylic Alkylations	14
1.3 Tungsten Mediated Allylic Alkylations	18
1.4 Molybdenum Mediated Allylic Alkylations	21
1.5 Cobalt Mediated Allylic Alkylations	23
1.6 Iron Mediated Allylic Alkylations	24
2 Results And Discussion	29
2.1 The $\text{Fe}(\text{CO})_2(\text{NO})_2$ Alkylation Reactions	29
2.1.1 General Experimental Conditions for Alkylation Reactions . . .	29
2.1.2 The Allylic Chlorides	30
2.1.3 The Allylic Acetates	39
2.2 $\text{Fe}(\text{CO})_3(\text{NO})^- \text{Na}^+$ Alkylation Reactions With Geranyl Acetate	43
2.3 Possible interactions between $\text{Fe}(\text{CO})_3(\text{NO})^- \text{Na}^+$ and $\text{Fe}(\text{CO})_2(\text{NO})_2$	49
2.4 Conclusion	54

3	Experimental Section	56
3.1	General	56
3.2	Preparation of the Dimethyl Malonate Anion, NaDMM	57
3.3	Preparation of the Acetates	57
3.3.1	crotyl acetate	57
3.3.2	α -methyl allyl acetate	58
3.3.3	geranyl acetate	58
3.3.4	neryl acetate	59
3.3.5	cinamyl acetate	59
3.3.6	α -phenyl allyl acetate	59
3.4	Preparation of Iron Compounds	60
3.4.1	Iron Dinitrosyl Dicarbonyl, $\text{Fe}(\text{CO})_2(\text{NO})_2$	60
3.4.2	Sodium Tricarbonylnitrosyl Iron Methanolalate; $\text{Fe}(\text{CO})_3\text{NO}^- \text{Na}^+ \cdot \text{CH}_3\text{OH}$	60
3.4.3	Sodium Tricarbonylnitrosyl Iron-1,4 Dioxanalate ; $\text{Fe}(\text{CO})_3(\text{NO})^- \text{Na}^+ \cdot 1,4\text{-dioxane}$	61
3.5	GC Calibration Curves	61
3.5.1	crotyl-DMM	61
3.5.2	α -methyl allyl-DMM	62
3.5.3	geranyl-DMM	63
3.6	$\text{Fe}(\text{CO})_2(\text{NO})_2$ Alkylation Reactions	64
3.6.1	General Experimental for Alkylation Reactions	64
3.6.2	Alkylation of Allylic Chlorides	65
3.6.3	The Allylic Acetates	70
3.7	The $\text{Fe}(\text{CO})_3(\text{NO})^-$ Alkylation Reactions With Geranyl Acetate . . .	77

3.7.1	$\text{Fe}(\text{CO})_3(\text{NO})^- \text{Na}^+ \cdot \text{MeOH}$	77
3.7.2	$\text{Fe}(\text{CO})_3(\text{NO})^- \text{Na}^+$ In Situ	80
3.7.3	$\text{Fe}(\text{CO})_3(\text{NO})^- \text{Na}^+ \cdot 1,4\text{-dioxane}$	80
3.8	$\text{Fe}(\text{CO})_3(\text{NO})^- \text{Na}^+$, Allyl Acetate Reaction	82
3.9	Reactions with $\text{Fe}(\text{CO})_2(\text{NO})_2$, $\text{Fe}(\text{CO})_3(\text{NO})^- \text{Na}^+$, and Geranyl Acetate	82
Bibliography		86

List of Figures

1.1	Displacement reactions with and without the mediation of transition metal complexes.	13
1.2	The suggested mechanism for the activation of the allylic position of an olefin by palladium (II) salts.	15
1.3	Conversion of a Pd(II) chloride dimer to a cationic π -allyl palladium moiety followed by a catalytic reaction.	15
1.4	A catalytic reaction path using a palladium (0) complex.	16
1.5	The co-ordination of a palladium(0) complex to an olefin.	17
1.6	A comparison of the regioselectivities when the steric demands of the nucleophile are increased.	19
1.7	Molecular orbital calculations were carried out on the phenylpentadienyl cation in order to probe the intrinsic bias for nucleophile attack on the cation itself in the absence of any steric or metal effects.	20
1.8	The stereochemistry of the W-catalyzed allylic alkylation.	20
1.9	An example of the chemoselective possibilities of W catalyzed allylic alkylations	21
1.10	Alternative sites for nucleophilic attack on an unsymmetrical olefin-Mo complex	22
1.11	Chemoselectivity and regioselectivity are exemplified in the Mo-catalyzed alkylation of 3-acetoxy-5-carbomethoxy-cyclohex-1-ene.	23

1.12	Reaction of the acyl- π -allyl cobalt complex with stabilized carbanions results in alkylation at the unsubstituted π -allyl terminus.	24
1.13	The suggested model by Nicholas et al. for $\text{Fe}_2(\text{CO})_9$ mediated allylic alkylation.	25
1.14	The suggested model by Xu et al. for the $\text{Bu}_4\text{N}(\text{Fe}(\text{CO})_3\text{NO})$ mediated allylic alkylation	26
1.15	Mononitrosyl carbonyl iron complexes can be easily decomposed into dinitrosyl iron species as is exemplified by reactions Rc1 and Rc2 . . .	28
2.1	The IR spectra of a solution containing $\text{Fe}(\text{CO})_2(\text{NO})_2$, α -methyl allyl chloride, and NaDMM.	33
2.2	Some possible structures resulting from the interaction of $\text{Fe}(\text{CO})_2(\text{NO})_2$ and NaDMM.	36
2.3	Postulated $\text{Fe}(\text{CO})_2(\text{NO})_2$, NaDMM nucleophilic substitution reaction.	36
2.4	The $\text{Fe}_2(\text{CO})_9$ and NaDMM interaction intermediates postulated by Nicholas	39
2.5	A plot of the product formation versus time with the substrates $\text{Fe}(\text{CO})_3(\text{NO})^- \text{Na}^+$ (52%), NaDMM, and geranyl acetate	45
2.6	Postulated formation of an intermediate X from $\text{Fe}(\text{CO})_3(\text{NO})^- \text{Na}^+$	47
2.7	A series of IR spectra over time, of a reaction with the following reactants: $\text{Fe}(\text{CO})_3(\text{NO})^- \text{Na}^+$ (25%), NaDMM, and allyl acetate.	50
2.8	A plot of the GC product peak area ratios versus time with the substrates $\text{Fe}(\text{CO})_3(\text{NO})^- \text{Na}^+$ (25%), NaDMM, and allyl acetate.	51

2.9 Postulated interaction of species X with $\text{Fe}(\text{CO})_3(\text{NO})^- \text{Na}^+$ to form
species Y. 52

List of Tables

2.1	Results of $\text{Fe}(\text{CO})_2(\text{NO})_2$ mediated allylic chloride alkylations.	31
2.2	IR data of relevant compounds in the allylic alkylation reactions.	34
2.3	Regio and stereoselectivity of nucleophilic addition or allylic alkylation with NaDMM obtained by Nicholas.	38
2.4	Results of $\text{Fe}(\text{CO})_2(\text{NO})_2$ mediated methyl-allyl acetate alkylation reactions.	41
2.5	Results of $\text{Fe}(\text{CO})_2(\text{NO})_2$ mediated allylic acetate alkylation reactions.	42
2.6	Regioselectivity data for various metal mediated allylic alkylation reactions with crotyl acetate as the allylic substrate and DMM as the nucleophile.	42
2.7	Results of $\text{Fe}(\text{CO})_3(\text{NO})^- \text{Na}^+$ mediated geranyl acetate alkylation reactions.	46
2.8	Results of $\text{Fe}(\text{CO})_2(\text{NO})_2$ and/or $\text{Fe}(\text{CO})_3(\text{NO})^- \text{Na}^+$, geranyl acetate reactions.	52
3.1	crotyl-DMM gas chromatograph calibration curves.	62
3.2	α -methyl allyl-DMM gas chromatograph calibration curves.	63
3.3	geranyl-DMM gas chromatograph calibration curves.	64
3.4	NMR data of the products of the various allylic alkylation reactions.	66

3.5	Values for the plot of the disappearance of starting material and appearance of products over time for reaction e29.	77
3.6	Values for the plot of the disappearance of starting material and appearance of products over time for reaction e41.	82

Chapter 1

Introduction

1.1 Transition Metal Mediated Catalytic Allylic Alkylation

The aim of this chapter is to briefly outline the latest developments in transition metal mediated catalytic allylic alkylations.

Under a variety of conditions a number of π -allylmetal complexes react stoichiometrically with nucleophiles at the π -allyl ligand, resulting in transfer of the allyl group from the metal to the nucleophile. The π -allyl complexes of palladium have been extensively studied and used in organic synthesis [1,2,3,4]. π -Allyl complexes of other metals have been studied much less in their reactions with nucleophiles, these metal complexes offer an opportunity to provide new possibilities for selectivity in organic reactions. Selectivity can be subdivided into three major categories, chemo, regio, and stereoselectivity [5].

Chemoselectivity refers to functional group differentiation. In a molecule there are various types of bonds and the ability to recognize the different intrinsic reactivity of each bond type is of primary concern. Thus, the differentiation between an alkene and a carbonyl group is a problem of chemoselectivity.

Regioselectivity deals with the orientation control at a single reaction center.

When a reagent and/or a substrate are unsymmetrical, their orientation with respect to each other is a problem of regioselectivity. Examples of this are the Markovnikov or the anti-Markovnikov additions to an alkene, the position of the substitution in aromatic rings, and the positions of alkylation of unsymmetrical ketones.

The third major category is associated with reaction at a given site and is a question of stereochemical control. If there exists only one chiral center in the substrate molecule, then induction of one of the two possible antipodes at the reaction center controls the absolute stereochemistry. This is called enantioselectivity. If there exist other chiral centers in the substrate molecule, control of the relative stereochemistry at the reaction center compared to those chiral centers is a problem of diastereoselectivity.

Allylic acetates and sulphones are relatively unreactive allylic derivatives and are not considered to be alkylating agents. In a typical displacement reaction the allylic acetates (fig.1.1, path (i)) [5] undergo bromide displacement. However, in the presence of certain transition metal complexes, the chemoselectivity can be changed. Thus is the case for paths ii and iii of figure 1.1. In the presence of the indicated complex, the bromide is unaffected and the acetate group becomes the leaving group.

In considering the question of regioselectivity of allylic alkylations, there are five factors [6] which could affect the regioselectivity: (1) steric demands of the nucleophile, (2) steric demands of the π -allyl substituents, when they are intermediates, (3) charge distribution of the π -allyl intermediate, (4) steric and electronic demands of the metal complex, and (5) reactivity of the nucleophile. Since factors (3) and (4) are determined by the metal complex, variation of the metal complex and its attendant ligands one can favor one or the other of the allyl termini. (See fig.1.1, path (ii) and (iii).)

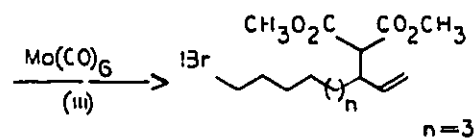
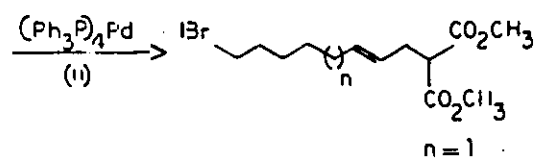
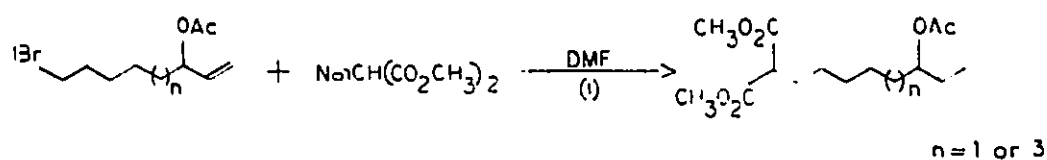


Figure 1.1: In a typical displacement reaction the allylic acetates (path (i)) undergo bromide displacement. However, the addition of a transition metal, which can coordinate the alkene and initiate ionization, specifically activates the allylic acetate. The bromide is not affected even though it is a much better leaving group (path (ii) and (iii)).

The following sections will deal with palladium, tungsten, molybdenum, cobalt, and iron catalytic allylic alkylations. This is in no way a review of all metal mediated allylic alkylations. Notable exceptions are Ni [7,8], Rh [9], Ru [9], and Cu [10].

1.2 Palladium Mediated Allylic Alkylations

The activation of the allylic position of an olefin can be achieved by palladium (II) salts. Nonconjugated olefins react faster, enones also form the desired complexes [11]. The reaction conditions may be tempered considerably [12] by changing the electrophilic nature of the Pd (II) salt. The regioselectivity is generally in accord with a Markovnikov-like process. The suggested mechanism of the reaction is as outlined in figure 1.2 and appears to involve a palladium hydride species [13]. Activation and subsequent loss of the hydrogen at the position allylic to the more substituted end of the olefin can be rationalized in terms of the olefin-palladium complex resonance forms whereby the build up of positive character occurs at the more substituted olefinic carbon.

The π -allylpalladium complexes are electrophilic conjunctive reagents [14] and as such can undergo alkylation with appropriate nucleophiles. The most common of these nucleophiles is a stabilized anion (conjugate acid with a $pK_a \sim 10-20$), for example, sodium dimethylmalonate.

The electrophilicity of the usual π -allylpalladium chloride-bridged dimers is not usually sufficient to initiate allylic alkylation. The complexes normally require activating ligands such as phosphines [15]. This converts the chloride-bridged dimers to π -allylpalladium cationic complexes [16]. The nucleophile attacks the cationic π -allyl moiety on the face opposite to that of palladium thus giving a normal inversion of configuration at carbon, with palladium (0) becoming the leaving group (fig.1.3). The

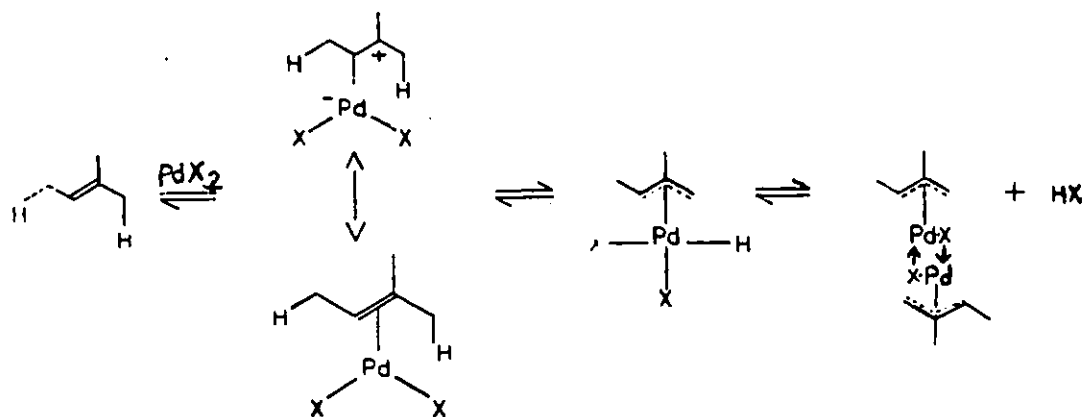


Figure 1.2: The suggested mechanism for the activation of the allylic position of an olefin by palladium (II) salts.

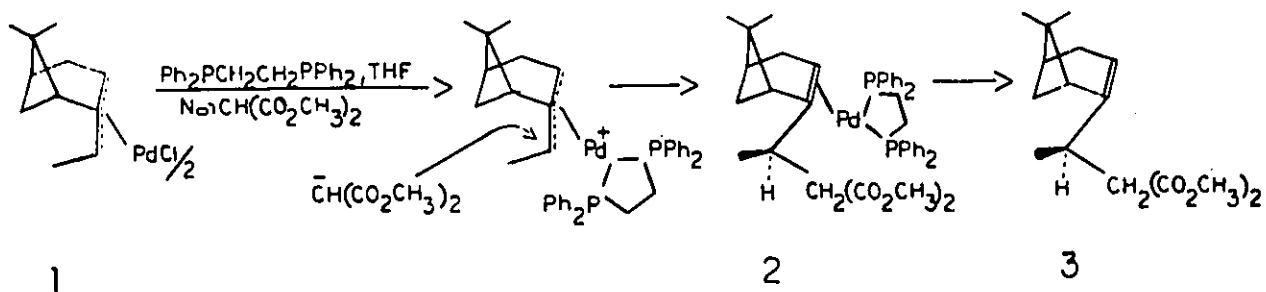


Figure 1.3: The π -allylpalladium chloride-bridged dimers are usually not sufficiently electrophilic to initiate allylic alkylation. They require activating ligands such as phosphines to convert the chloride-bridged dimers to π -allylpalladium cationic complexes. The nucleophile then attacks the cationic π -allyl moiety on the face opposite to that of palladium thus giving a normal inversion of configuration at carbon, with palladium (0) becoming the leaving group.

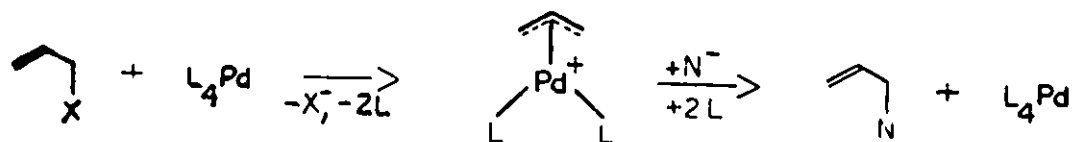


Figure 1.4: A catalytic reaction path using a palladium (0) complex.

stereochemistry of the alkylation product reflects the stereochemistry of the π -allyl complexes in which the syn complexes are preferred to the anti-complexes. Since both the E and Z olefins form the same π -allyl complex (because of thermodynamic control), the resulting E olefin synthesis is stereocontrolled. Finally, high regioselectivity is observed when the nucleophile bonds to the less substituted carbon.

In a study conducted by Julia et al. [17] the influence of the leaving groups, the carbanions, and the ligands on π -allyl palladium in the substitution of primary or tertiary terpene derivatives is investigated. The regio and stereoselectivity as well as the overall yields of the reactions are strongly influenced by the carbanions and the ligands on the π -allyl palladium.

The potential for developing a catalytic procedure involving nucleophilic attack on an olefin-palladium (II) complex appears limited to the simplest olefins. In addition, there is a very low turnover for palladium [18]. However, if a palladium (0) complex is used, an alternative catalytic reaction path is possible. This is outlined in figure 1.4. With the use of an appropriate leaving group in the allylic position and a palladium (0) complex to initiate ionization, an intermediate similar to the stoichiometric process is obtained. Nucleophilic attack yields the allylic alkylation products and regenerates the palladium (0) complex. Typical catalysts include tetrakis(triphenylphosphine) palladium and bis(1,2 - bis(diphenylphosphino) ethane) palladium.

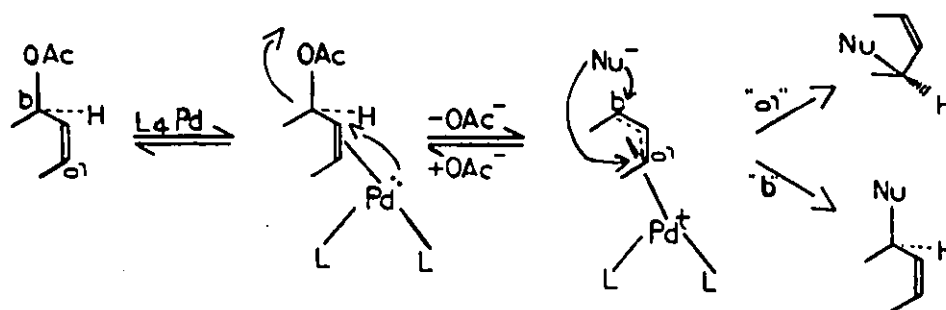


Figure 1.5: The co-ordination of the palladium (O) complex to the olefin occurs on the face distal to the leaving group. Palladium displaces the acetate with inversion to give the π -allyl complex. The nucleophile attacks the π -allyl cationic complex on the face opposite to that occupied by palladium at either site "a" or site "b" with inversion. This double inversion creates a net retention for this alkylation process but the regioisomeric nature of the starting material is lost.

A likely mechanistic path is summarized in figure 1.5. The co-ordination of the palladium (O) complex to the olefin occurs on the face distal to the leaving group. Palladium displaces the acetate with inversion to give the π -allyl complex. The nucleophile attacks the π -allyl cationic complex on the face opposite to that occupied by palladium at either site "a" or site "b" with inversion. This double inversion creates a net retention for this alkylation process. The regiochemistry of the product is determined by a combination of factors such as the nature of the nucleophile, the nature of the substituent on the π -allyl unit, and the nature of the ligands on palladium.

The nature of the leaving group has not been extensively studied. The usual leaving group used has been an acyloxy such as acetate. Acyl ethers and hydroxyl groups have served as leaving groups but are less satisfactory than acyloxy. The use of sulfur containing leaving groups such as sulphones provide versatility [19].

The range of possible nucleophiles which could be useful remains undefined with the stabilized anions being the most often used. Less stabilized nucleophiles such as complex enolates are known to react successfully.[20] Enol stannanes react rapidly

and in high yield to give the derived C-alkylated product in a highly chemoselective and regioselective fashion.[21,22,23]

Palladium complexes could be used as conformational control reagents in conformationally nonrigid systems [24]. As well, the use of chiral phosphines as ligands has resulted in asymmetric induction [25].

1.3 Tungsten Mediated Allylic Alkylations

In the development of a tungsten catalyzed allylic alkylation, allyl acetate and sodium dimethylmalonate was used in the test reaction [6]. It was found that $W(CO)_6$ had no catalytic activity but that $(CH_3CN)_3 W(CO)_3$ did lead to a slow reaction (31% in 16h). The addition of phosphates poisoned the catalyst, but the use of a stronger σ -donor type ligand such as bpy (2,2'-bipyridyl), to facilitate the opening of a coordination site on the tungsten, did lead to a significant improvement (65% in 18h). When carbonate was substituted for acetate, a more general reaction was obtained with a better yield (81% in 12h).

The best reaction yields were obtained when the allyl substrates bore one aryl group. Alkylation occurred predominantly at the more substituted end regardless of the nucleophile. There was some decrease in regioselectivity when the steric demands of the nucleophile were increased. A comparison of the results in figure 1.6 illustrates the effect of the aromatic ring on regioselectivity [6]. In the case of the alkyl-substituted π -allyl group, steric demands of the nucleophile compete with the steric demands of the metal complex to dominate the regioselectivity.

Molecular orbital calculations [26] were carried out on the phenylpentadienyl cation (this can be viewed as an allyl cation bonded to a zero valent metal) in order to probe the intrinsic bias for nucleophile attack on the cation itself in the absence

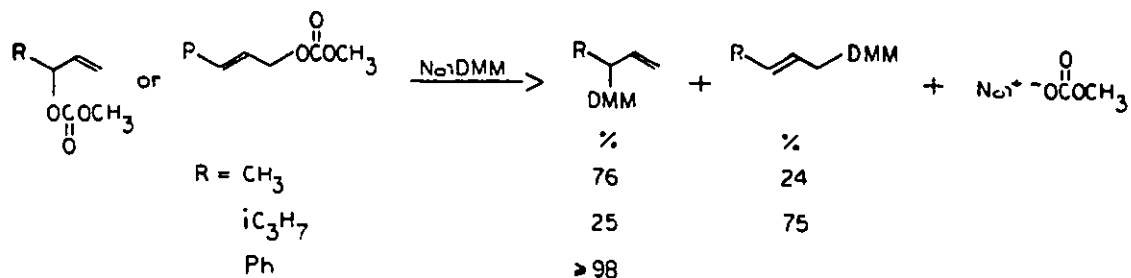


Figure 1.6: A comparison of the regioselectivities when the steric demands of the nucleophile are increased.

of any steric or metal effects.

On the basis of charge considerations, the order of attack should be $C(1) \sim C(3) > C(5)$. The same order is predicted by computing the LUMO coefficients of the allylic carbons.

To test these predictions a few assumptions were made: the complexes are η^3 species, there is an absence of any Michael-type additions, and the equilibration of the two regioisomeric η^3 complexes is slow relative to alkylation. On the basis of charge and frontier orbital considerations, complex A (fig. 1.7) [26] should alkylate at C(3) and complex B almost equally at C(1) and C(3).

The experimental results using the W-catalyzed alkylation are in very good accord with the MO predictions. These results strongly support the notion that the W-catalyzed reactions reflect the intrinsic electronic bias of the η^3 - allyl system.

The stereochemistry of the W-catalyzed allylic alkylation is the same as observed with molybdenum and palladium catalysts, fig. 1.8 [6].

The chemoselective possibilities are exemplified by the following: linalyl methyl carbonate alkylates smoothly but geranyl methyl carbonate only gives trace amounts of product after 47 hours [6]. This suggests that the ionization step is dependent on the degree of substitution of the carbon bearing the leaving group. This can be used

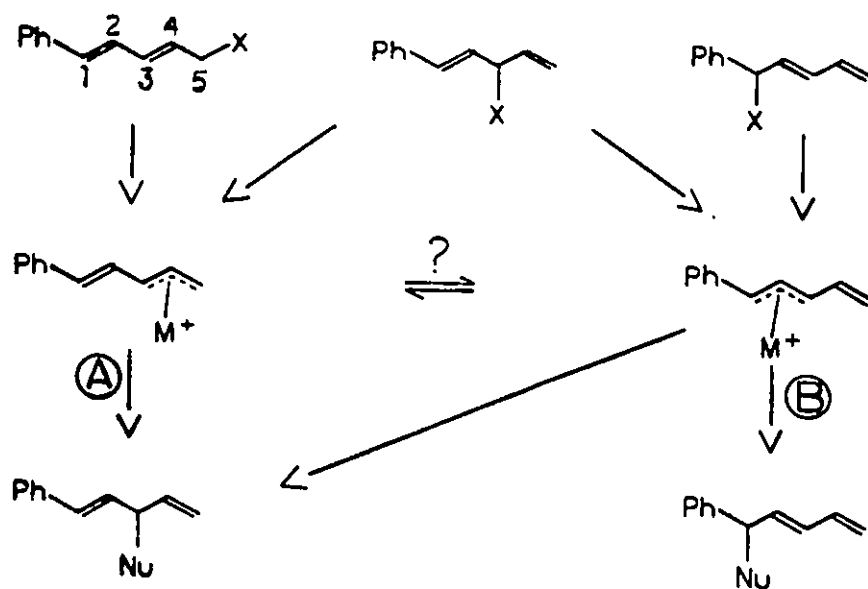


Figure 1.7: Molecular orbital calculations were carried out on the phenylpentadienyl cation in order to probe the intrinsic bias for nucleophile attack on the cation itself in the absence of any steric or metal effects.

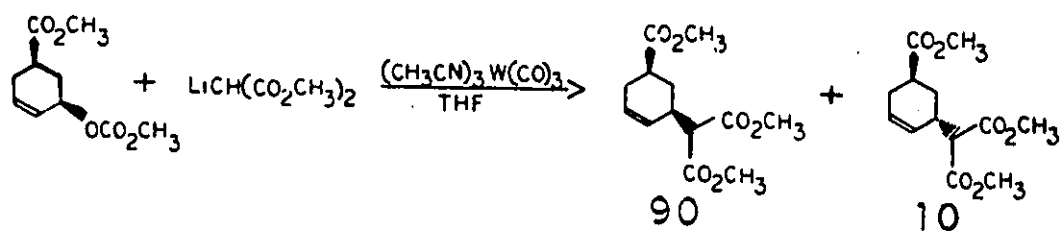


Figure 1.8: The stereochemistry of the W-catalyzed allylic alkylation.

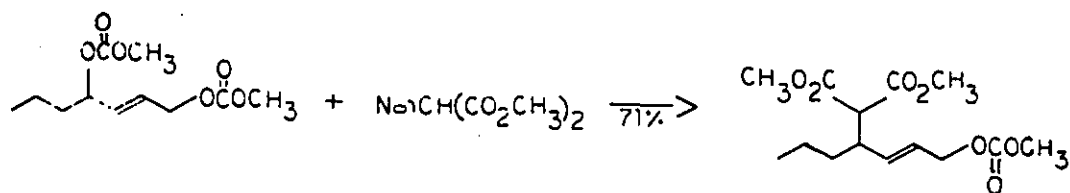


Figure 1.9: An example of the chemoselective possibilities of W catalyzed allylic alkylations

to an advantage as demonstrated in figure 1.9 [6]. The tungsten catalyst permits easy replacement of the secondary carbonate without affecting the primary carbonate for the limited reaction times employed (5h). The high regioselectivity of this alkylation presumably reflects the effects of polar substituents to direct the incoming nucleophile to the more distant allyl terminus.

1.4 Molybdenum Mediated Allylic Alkylations

The interest in the development of molybdenum catalyzed allylic-alkylation reactions is spurred by the ready availability of π -allylmolybdenum complexes, its high coordination number, and the lack of information regarding the susceptibility toward nucleophilic attack of the allyl ligand.

Reaction of allylic acetates [27] with the anion of dimethylmalonate or 2-carbomethoxy-cyclopentanone was performed in the presence of $\text{Mo}(\text{bpy})(\text{CO})_4$, $\text{Mo}(\text{dppe})(\text{CO})_4$, $\text{Mo}(\text{TMEDA})(\text{CO})_4$ or $\text{Mo}(\text{CO})_6$ with $\text{Mo}(\text{CO})_6$ being preferred. $\text{Mo}(\text{bpy})(\text{CO})_4$ and $\text{Mo}(\text{CO})_6$ have complimentary regiochemical behavior although this may be modified by the steric demands of the nucleophile. The variation in the regioselectivity between different nucleophiles does not appear to stem from different catalysts (although some new catalysts may be generated when different solvents are used) [27] but rather from an intrinsic balance among reactivity of the anion, its

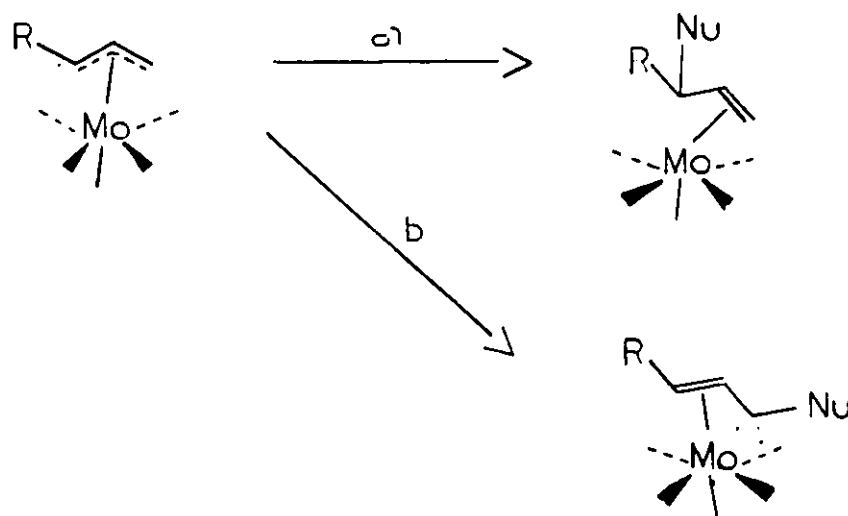


Figure 1.10: Alternative sites for nucleophilic attack on an unsymmetrical olefin-Mo complex

steric demands, the charge distribution in the intermediate π -allyl system, and the stability of the resultant olefin and the olefin-metal complex [28]. In an unsymmetrical complex such as found in figure 1.10 [28], the C(1) carbon would be more electron deficient than the terminal C(3).

Attack at C(1) leads to the sterically and electronically preferred olefin-Mo complex. If the nucleophile has a high reactivity but with minimum steric requirements, then path A is preferred. If the nucleophile is not very reactive and has steric demands sufficiently important, then path B will totally dominate.

Chemoselectivity and regioselectivity are exemplified in the alkylation of 3-acetoxy-5-carbomethoxy-cyclohex-1-ene (fig.1.11) [27].

The Mo(bpy) catalyst gives the same results as the corresponding palladium catalyzed reaction. The molybdenum catalyzed allylic-alkylation reaction shows great regiochemical control by varying either the ligands or the nucleophiles. There is a higher selectivity for attack at the primary carbon as opposed to the secondary carbon of the π -allyl fragment. One drawback with respect to palladium catalyzed reactions is that the molybdenum reactions require higher temperatures and longer

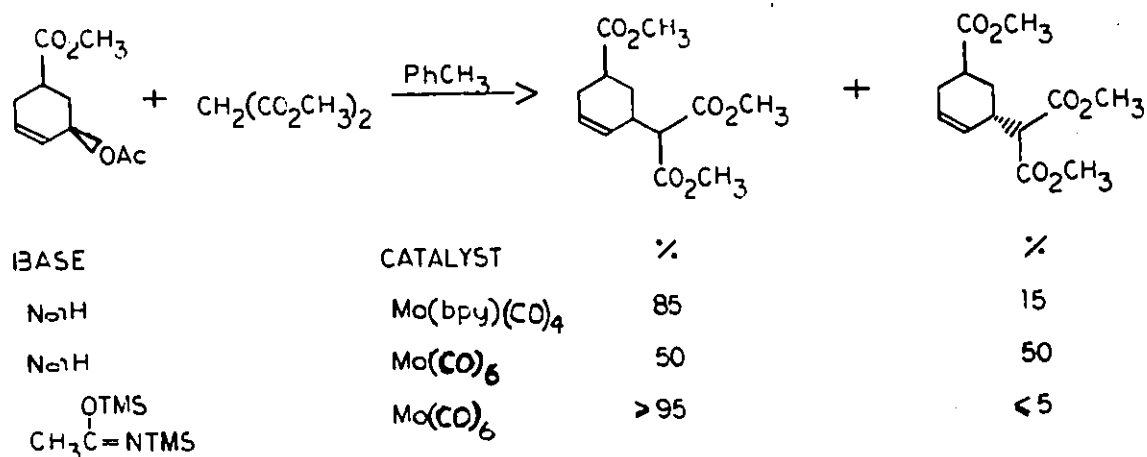


Figure 1.11: Chemoselectivity and regioselectivity are exemplified in the Mo-catalyzed alkylation of 3-acetoxy-5-carbomethoxy-cyclohex-1-ene.

reaction times.

1.5 Cobalt Mediated Allylic Alkylations

Stoichiometric cobalt allylic alkylation was developed by utilizing the prior knowledge gained in the study of π -allyl cobalt and acyl cobalt complexes. Acyl- π -allyl cobalt complexes were prepared by reacting $\text{NaCo}(\text{CO})_4$ and organic halides with butadiene, isoprene or allene [29]. Reaction of each respective acyl- π -allyl cobalt complex (fig. 1.12) [29] with stabilized carbanions results in alkylation at the unsubstituted π -allyl terminus. The procedure provides an overall 1,4-acylation/alkylation of 1,3-dienes in which three carbon-carbon bonds are formed in a one pot, four step reaction sequence. The overall yields of this acylation/alkylation reaction are only modest but with four steps involved, assuming the mechanism is correct, the overall process is reasonably efficient.

Studies by Roustan et al. [30] using η^3 -crotyl cobalt tricarbonyl have shown that

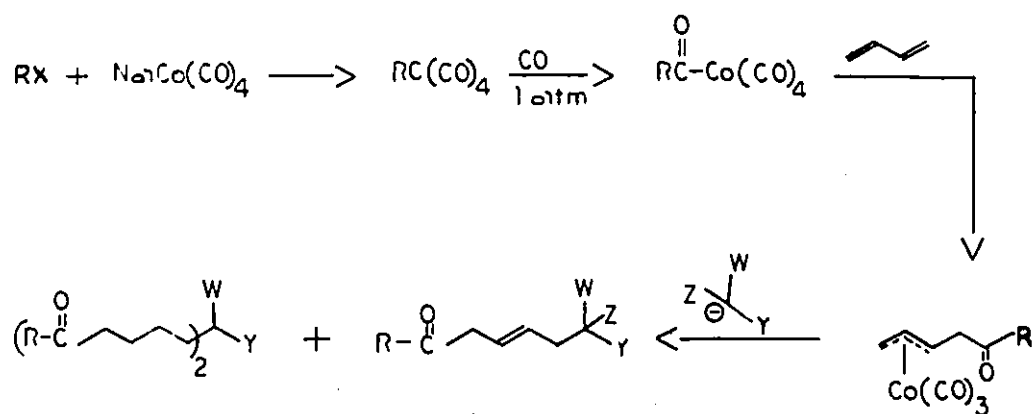


Figure 1.12: Reaction of the acyl- π -allyl cobalt complex with stabilized carbanions results in alkylation at the unsubstituted π -allyl terminus.

although the regioselectivity was initially poor it could be ameliorated by substituting a carbonyl ligand with a phosphine ligand. It should be noted that this is the only group to have reported catalytic cobalt mediated allylic alkylation reactions.

The regioselectivity of alkylation indicates a bias for attack at the unsubstituted π -allyl terminus but the initial site of nucleophilic attack on the π -allylcobalt complex is not known. Upon addition of the carbanion to the π -allyl cobalt tricarbonyl solution, the solution turns deep red which gradually fades to a pale yellow over the course of the reaction [29]. This could imply the formation of some internal intermediate complex.

1.6 Iron Mediated Allylic Alkylations

In work carried out by Nicholas et al. [31] the catalytic activity of $\text{Fe}_2(\text{CO})_9$ was examined. It was found that in the coupling of NaDMM with $(\eta^3\text{-crotyl})\text{Fe}(\text{CO})_4\text{BF}_4$ and crotyl acetate, preferential attack occurred at the less substituted allyl termi-

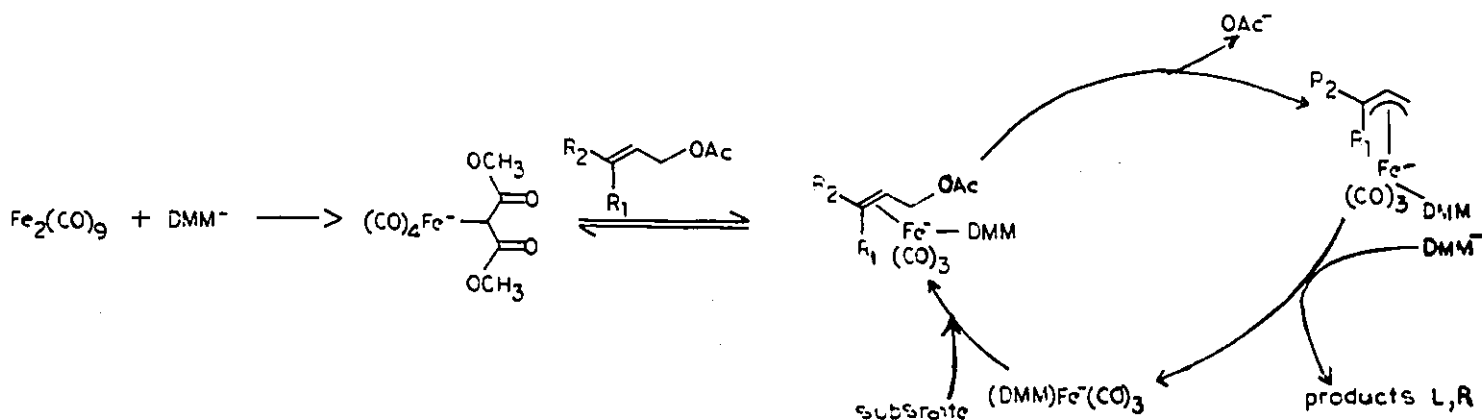


Figure 1.13: The suggested model by Nicholas et al. for Fe₂(CO)₉ mediated allylic alkylation.

nus and thus stereospecifically. The allyl fragment's original geometry was thus retained. With (η^2 -crotyl-OAc)Fe(CO)₄, a lesser preference for attack at the primary carbon was exhibited but the reaction did proceed stereospecifically. Coupling of allylic acetates with nucleophiles catalysed by Fe₂(CO)₉ also proceeded with high stereospecificity but with generally lower regioselectivity than in the stoichiometric reactions. The regioselectivities resulting from the allylic alkylation catalysed by Fe₂(CO)₉ could not be attributed to the intermediacy of either the η^3 or η^2 complexes. Thus, a pathway not requiring the intermediacy of either the η^3 or η^2 complexes was postulated (see figure 1.13). Studies of the interaction of NaDMM with Fe₂(CO)₉ and the resulting IR and NMR data obtained have provided evidence for the formation of Fe_x(CO)_yDMM⁻ ions, in which DMM⁻ acts as a ligand towards iron, in the catalytic reactions and their involvement as precursors to the actual catalyst species.

Using Bu₄N(Fe(CO)₃NO), Xu et al. [32] have found that the alkylation of allylic carbonate with malonate anion proceeded catalytically with good regioselectivity

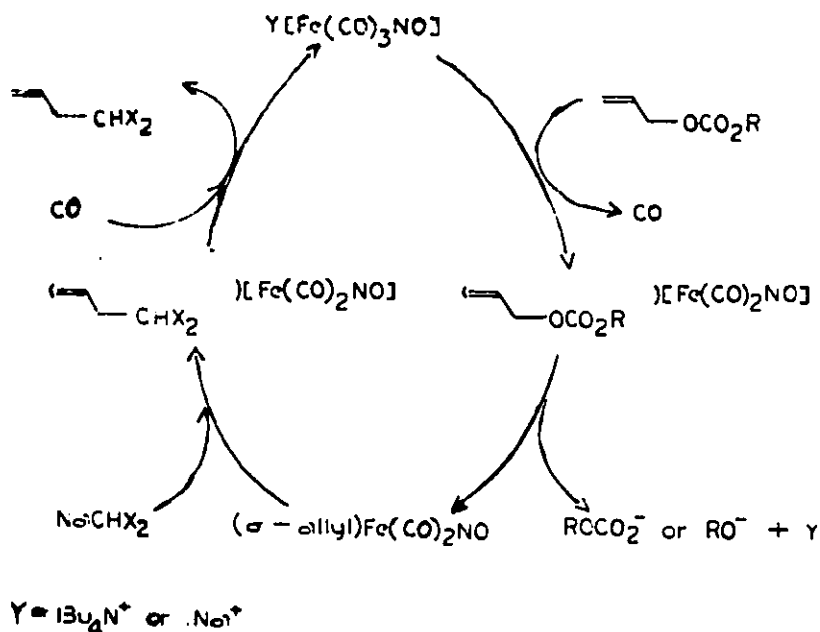


Figure 1.14: The suggested model by Xu et al. for the $\text{Bu}_4\text{N}(\text{Fe}(\text{CO})_3\text{NO})$ mediated allylic alkylation

and with the nucleophile attacking predominantly at the carbon where the leaving group was attached. This confirms previous studies with allylic acetates [30]. The stereoselectivity of the alkylation reaction was studied and retention of configuration of both the carbon centers undergoing substitution was found. A reaction pathway involving a σ -allyliron complex was suggested and is shown in figure 1.14. It is noteworthy that according to Xu, the $\text{Bu}_4\text{N}(\text{Fe}(\text{CO})_3\text{NO})$ mediated allylic alkylation did not take place in the absence of carbon monoxide. This is a puzzling report given the reaction pathway which requires, in the initial step, the substitution of a CO by the allylic substrate. The reaction should at least proceed stoichiometrically.

Prior to work reported by Nicholas, better regioselectivities were reported by Roustan et al. [32] with sodium tricarbonyl nitrosyl iron as an iron-based catalyst. It is indeed from this early work that was obtained the first evidence that complexes with metallic centers in a low oxidation state and in association with good to excellent

π -acid ligands might provide useful alkylation catalysts.

It has been shown that the iron complexes of $(\eta^3\text{-crotyl})\text{Fe}(\text{CO})_2\text{NO}$ and $\text{Fe}(\text{CO})_3\text{NO}^- \text{Na}^+$ have the ability to catalyze the alkylation of allylic substrates [30]. Alkylations by nucleophiles such as the diethylmalonate anion can be carried out in THF at room temperature with allylic chlorides. The regioselectivity is such that the nucleophile preferentially alkylates the carbon where the leaving group was initially attached, whether it be a primary or secondary carbon. This suggests that in the catalytic cycle (or cycles), the attack of the nucleophile takes place on a reaction intermediate other than a η^3 -allylic complex.

When an allylic chloride was reacted with NaDEM in the presence of $\text{Fe}(\text{CO})_3\text{NO}^-$, allylic alkylation occurred. The reaction was regioselective and catalytic (see table 2.1 for experimental results). Monitoring the reaction by IR did not reveal any intermediate formation. The initial $\text{Fe}(\text{CO})_3\text{NO}^-$ IR spectra remained seemingly unchanged throughout the reaction but this did not preclude intermediates.

With respect to the mechanisms of the $\text{Fe}(\text{CO})_3(\text{NO})^- \text{Na}^+$ mediated alkylations, at the time our work was undertaken, it could only be stated that the observed regioselectivities ruled out the involvement of η^3 -allyl intermediates in the predominant catalytic pathways. No information was available for delineating the nature of the active iron species. Among potential candidates, one could think of:

- 1) $\text{Fe}(\text{CO})_3(\text{NO})^- \text{Na}^+$ itself.
- 2) A metallic impurity systematically present in the samples of the reagent used, due to its method of preparation.
- 3) An iron species derived from $\text{Fe}(\text{CO})_3(\text{NO})^- \text{Na}^+$ by an in-situ reaction and in that case the anionic complex would serve only as the precursor of the active ones,

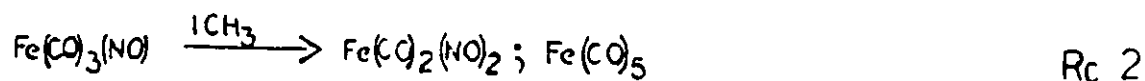
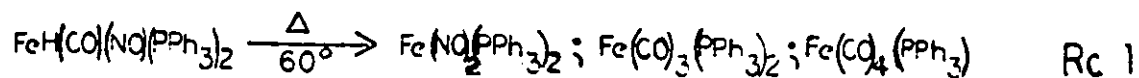


Figure 1.15: Mononitrosyl carbonyl iron complexes can be easily decomposed into dinitrosyl iron species as is exemplified by reactions Rc1 and Rc2

with no reversible relationship between the two.

With respect to the third possibility, it has been shown that mononitrosyl carbonyl iron complexes can be easily decomposed into dinitrosyl iron species. This is exemplified by reactions Rc1 [33] and Rc2 [41] in figure 1.15.

Of particular interest is reaction 2, in which $\text{Fe}(\text{CO})_2(\text{NO})_2$ is formed upon reaction of the nitrosyl anion with ICH_3 . The same dinitrosyl complex is also frequently observed as a by product in the synthesis of $(\eta^3\text{-allyl})\text{Fe}(\text{CO})_2(\text{NO})$ derivatives from $\text{Fe}(\text{CO})_3(\text{NO})^- \text{Na}^+$ and an allyl chloride.

These observations led us to study the catalytic activity of $\text{Fe}(\text{CO})_2(\text{NO})_2$ in allylic alkylations.

Chapter 2

Results And Discussion

2.1 The $\text{Fe}(\text{CO})_2(\text{NO})_2$ Alkylation Reactions

With $\text{Fe}(\text{CO})_2(\text{NO})_2$ targeted as the possible catalytic agent, a series of alkylation reactions with various allylic substrates was carried out.

2.1.1 General Experimental Conditions for Alkylation Reactions

This general experimental subsection presents an overview of the typical reaction conditions used for the alkylation reactions. This will provide the reader with the experimental context from which the results were obtained.

In a Schlenk tube under argon atmosphere, $\text{Fe}(\text{CO})_2(\text{NO})_2$ was dissolved in freshly distilled, argon saturated THF. The molar ratio of iron complex with respect to the allylic substrate was varied from 10 to 100%. To this clear red solution was added one equivalent (with respect to the allylic substrate) of the sodium dimethyl malonate anion (NaDMM), and the optional addition of dimethyl malonate (DMM). This was followed by the addition of one equivalent of the allylic substrate. With the chloro substituted allylic substrates, the mixture was stirred at room temperature, whereas, for the allylic acetates the solution was at THF reflux. The reaction time was varied from 0.5h to 72h. The reactions were monitored by observing both the

disappearance of the starting materials and the appearance of the products by IR and TLC. Of particular use in the determination of the completion of the reaction was the disappearance of the 1680cm^{-1} IR peak of NaDMM. The work-ups were carried out as follows: hydrolysing, extracting, drying and filtering. To the crude product mixture was added a known quantity of mesitylene, used as the internal standard for the gas chromatogram (GC) yields. A gas chromatogram was taken of this crude product and the GC yields were calculated using previously established standard curves. Some of the crude product mixtures were further purified by column chromatography, preparative thin layer chromatography, or by reduced pressure distillation. The isolated products were verified for purity by GC and characterized by either ^1H NMR, ^{13}C NMR, GC-MS, or a combination of these.

2.1.2 The Allylic Chlorides

In the study by Roustan et al. [30], the alkylation of crotyl chloride and α -methyl allyl chloride were carried out at room temperature in the presence of $\text{Fe}(\text{CO})_3(\text{NO})^- \text{Na}^+$. It seemed appropriate to begin with these same allylic chlorides in reactions at room temperature, but with $\text{Fe}(\text{CO})_2(\text{NO})_2$. In table 2.1 can be found a summary of the results obtained for the allylic chloride reactions with $\text{Fe}(\text{CO})_2(\text{NO})_2$, as well as, for comparison, the results obtained for $\text{Fe}(\text{CO})_3(\text{NO})^- \text{Na}^+$ (entries eF1 and eF2).

The regioselectivity of the allylic chlorides varied from fair to very good. For $\text{Fe}(\text{CO})_2(\text{NO})_2$ at 10% of crotyl chloride (entries e2, e4), regioselectivities of approximately 87% for crotyl-DMM (linear) and 13% for α -methyl allyl-DMM (ramified) were obtained. The α -methyl allyl chloride with 10% $\text{Fe}(\text{CO})_2(\text{NO})_2$ (entries e1, e3), although having approximately the same overall yield as the crotyl chloride, was much poorer in regioselectivity with crotyl-DMM at 39% and α -methyl allyl-DMM

<i>Fe(CO)₂(NO)₂, α-methyl allyl chloride</i>								
<i>Rx</i>	<i>%M</i>	<i>Rx time</i>	<i>%Nu</i>	<i>%DMM</i>	<i>GC %yield</i>	<i>Regioelec.</i>		<i>Comments</i>
						<i>Linear</i>	<i>Ramified</i>	
e1	10	1.5	100	0	60	37	63	Ar
e3	10	>2.5	100	0	55	40	60	CO
e5	100-10	38	100	0	57	35	65	CO
e6	17	32+40	100	0	22	40	60	Ar, CO, PPh ₃
e7	20	<1	110	100	89	19	81	
e9	10-80	8+50	100	0	64	33	67	
eF1	20	48	100(1)	100	90	18	82	Fe(CO) ₃ (NO) ⁻ Na
<i>Fe(CO)₂(NO)₂, crotyl chloride</i>								
e2	10	1.0	100	0	54	85	15	Ar
e4	10	2.5	100	0	57	88	12	CO
e8	20	<1	110	100	74	81	19	
eF2	20	48	100(1)	100	79	89	11	Fe(CO) ₃ (NO) ⁻ Na

Table 2.1: Results of Fe(CO)₂(NO)₂ mediated allylic chloride alkylations. %M=Molar percent metal with respect to allyl substrate. %Nu=Molar percent NaDMM with respect to allyl substrate. (1)eF1 and eF2 are results obtained by Roustan et al. [30] using NaDEM (sodium diethylmalonate) and Fe(CO)₃(NO)⁻Na⁺

at 61%. In going from 10 to 20 percent $\text{Fe}(\text{CO})_2(\text{NO})_2$, the overall yield and the regioselectivity increased significantly for both the linear and ramified allylic chloride alkylation reactions. The regioselectivities were 81%, 19% for crotyl chloride and 19%, 81% for α -methyl allyl chloride (see entries e8 and e7 respectively). Also, these increases were paralleled by decreases in reaction times.

For reactions e1 through e4, yields of greater than 10% in bisalkylation product with respect to the allyl substrate were obtained. But, as can be observed in reactions e7 and e8 (see Chapter 3, section 3.6.2), this high yield in bisalkylation product was reduced by adding an excess amount of DMM to the reaction mixture.

Comparing in table 2.1 the results obtained for the reactions performed with $\text{Fe}(\text{CO})_3(\text{NO})^- \text{Na}^+$ at 20% and those reactions performed with $\text{Fe}(\text{CO})_2(\text{NO})_2$ at 20%, one observes little difference in the regioselectivity but with a large time difference.

The results demonstrate that $\text{Fe}(\text{CO})_2(\text{NO})_2$ can form catalytically active species. Furthermore, in all cases the alkylation occurred predominantly at the carbon where the leaving group was attached.

When using the typical reaction conditions described for the allyl chlorides, the IR spectra (see figure 2.1) of a solution containing $\text{Fe}(\text{CO})_2(\text{NO})_2$, α -methyl allyl chloride, and NaDMM exhibited absorption peaks which could be attributed to the reactants and alkylation products, as well as peaks which could not be assigned.

A comparison of the known $\text{Fe}(\text{CO})_3(\text{NO})^- \text{Na}^+$ peak assignments (see table 2.2) with the 1880cm^{-1} and 1640cm^{-1} peaks observed in the spectra of figure 2.1 has led to a postulation that they are one and the same species. However, the $\text{Fe}(\text{CO})_3(\text{NO})^- \text{Na}^+$ peak usually observed in the 1977 to 1990cm^{-1} area was not seen given that the 1880cm^{-1} peak which is relatively much stronger was itself weak.

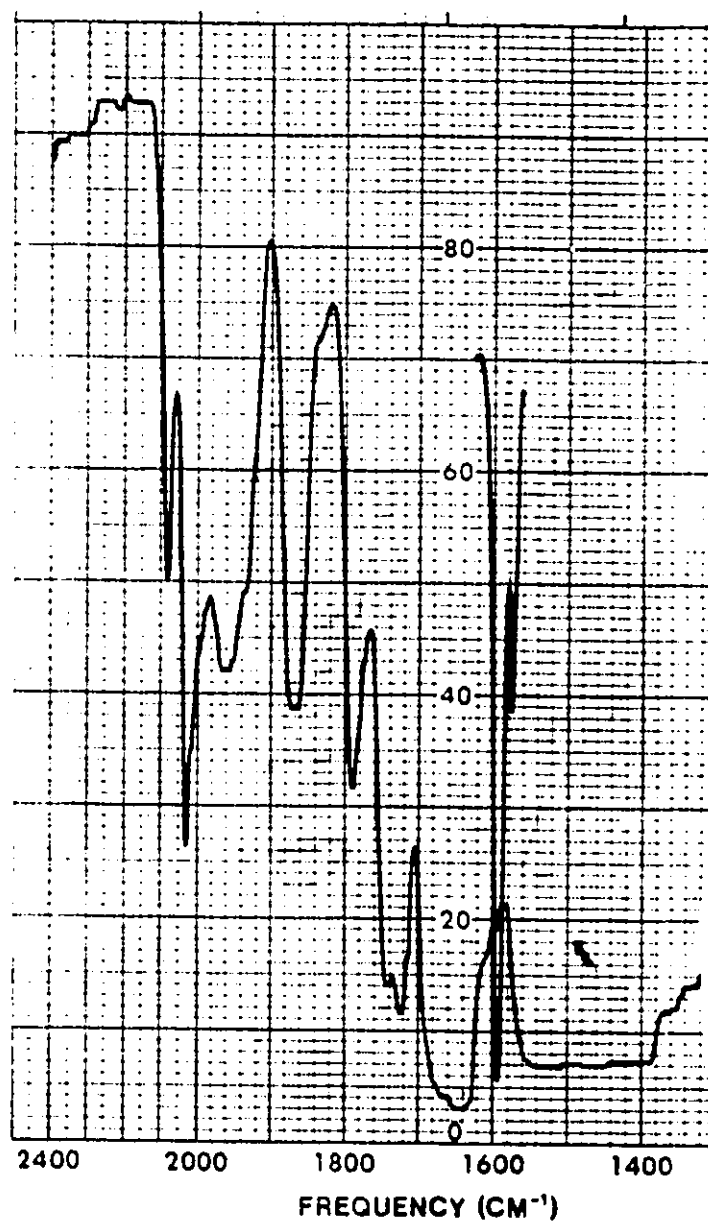


Figure 2.1: The IR spectra of a solution containing $\text{Fe}(\text{CO})_2(\text{NO})_2$, α -methyl allyl chloride, and NaDMM.

$Fe(CO)_2(NO)_2$ ^{(1)(a)}		
$\nu_{CO}(cm^{-1})$	2080(s), 2025(vs)	
$\nu_{NO}(cm^{-1})$	1810(s), 1760(vs)	
$Fe(CO)_3(NO)^- Na^+$ ^{(1)(b)}		
$\nu_{CO}(cm^{-1})$	1990(s), 1890(s); tight ion pair	
$\nu_{NO}(cm^{-1})$	1615(s)	
$\nu_{CO}(cm^{-1})$	1977(s), 1873(sh); loose ion pair	$Fe(CO)_3 NO^- Na^+$
$\nu_{NO}(cm^{-1})$	1648	\updownarrow $Fe(CO)_3 NO^- + Na^+$
$Fe(CO)(NO)_2(PPh_3)$ ^{(2)(c)}		
$\nu_{CO}(cm^{-1})$	1990(s)	
$\nu_{NO}(cm^{-1})$	1770(s), 1720(s)	
$(Fe(CO)(NO)_2DMM)^- Na^+$ ^{(1)(a)}		
$\nu_{CO}(cm^{-1})$	1970	
$\nu_{NO}(cm^{-1})$	1730, 1690	
$(Fe(CO)_4DMM)^- PPN^+$ ^{(2)(d)}		
$\nu_{CO}(cm^{-1})$	2025(m), 1985(m), 1960(w), 1920(s), 1900(s), 1703(m)	
DMM ^{(1)(a)}		
$\nu_{CO}(cm^{-1})$	1760, 1740	
$NaDMM$ ^{(1)(a)}		
$\nu_{CO}(cm^{-1})$	1680(s)	

Table 2.2: IR data of relevant compounds in the allylic alkylation reactions. (1)in THF, (2) in CH_2Cl_2 . (a)This work (b)Ref.[37] (c)Ref.[34] (d)Ref.[31]

The assignment of the 1970cm^{-1} and 1730cm^{-1} peaks to a given structure was not as straight forward as the $\text{Fe}(\text{CO})_3(\text{NO})^- \text{Na}^+$ peak assignments. The 1970cm^{-1} peak could be due to a species resulting from an interaction of $\text{Fe}(\text{CO})_2(\text{NO})_2$ with either α -methyl allyl chloride or NaDMM. The 1730cm^{-1} peak could be associated with the 1970cm^{-1} peak species, the product α -methyl allyl-DMM, or DMM.

In order to resolve this ambiguity, experiment e9 was performed. A series of 0.1 equivalent aliquots of $\text{Fe}(\text{CO})_2(\text{NO})_2$ were added to a 1.0 equivalent solution of NaDMM. With the first addition, the IR showed the formation of a peak at $\sim 1730\text{cm}^{-1}$. The growth in the 1970cm^{-1} and 1880cm^{-1} peaks was concomitant with the decrease in the $\text{Fe}(\text{CO})_2(\text{NO})_2$ peak. After 30 minutes of stirring the $\text{Fe}(\text{CO})_2(\text{NO})_2$ disappeared and the 1880cm^{-1} peak was larger than the 1970cm^{-1} peak. With the addition of four subsequent aliquots, the 1880cm^{-1} peak increased only slightly; the 1970cm^{-1} and the 1730cm^{-1} peaks continued to grow. The 1670cm^{-1} NaDMM peak did not change in peak intensity but did acquire a slight shoulder at 1690cm^{-1} . There was no marked transition between each successive addition. After the fifth addition, however, there was a slight amount of $\text{Fe}(\text{CO})_2(\text{NO})_2$ present after one hour of stirring and even more after a total of 7 additions.

From experiment e9, it is postulated that the peak formations observed in the IR of the reaction intermediates are the result of an interaction between $\text{Fe}(\text{CO})_2(\text{NO})_2$ with NaDMM. As stated, the 1880cm^{-1} peak has been assigned to $\text{Fe}(\text{CO})_3(\text{NO})^- \text{Na}^+$. The 1970cm^{-1} , 1730cm^{-1} and 1690cm^{-1} peaks need still to be assigned. A very likely structure for an intermediate having the above IR features is $(\text{Fe}(\text{CO})(\text{NO})_2\text{DMM})^- \text{Na}^+$ (see figure 2.2 A) with the ν (Fe-CO) at 1980cm^{-1} , ν (FeCH-CO-COCH₃) at 1730cm^{-1} , and one of the ν (Fe-NO)s at 1690cm^{-1} . This intermediate resulting from a DMM⁻ for CO substitution of $\text{Fe}(\text{CO})_2(\text{NO})_2$ according

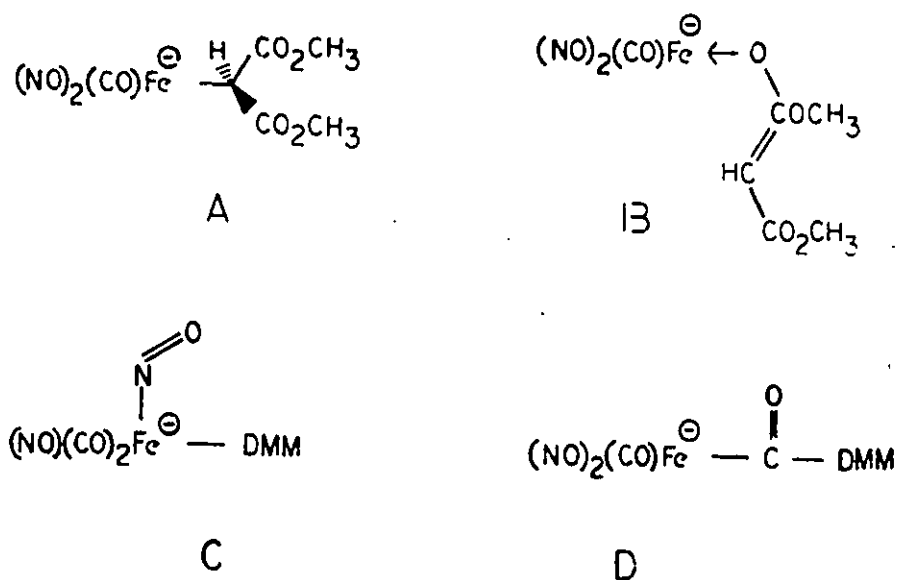


Figure 2.2: Some possible structures resulting from the interaction of $\text{Fe}(\text{CO})_2(\text{NO})_2$ and NaDMM .



Figure 2.3: Postulated $\text{Fe}(\text{CO})_2(\text{NO})_2$, NaDMM nucleophilic substitution reaction.

to figure 2.3.

A comparison of reaction e4, which was carried out under CO , with reaction e2, which was carried out under argon (table 2.1), shows that in the presence of CO there is a significant increase in reaction times. This is as expected for reaction A (figure 2.3) as written.

To verify whether or not there is an equilibrium in reaction 2.3, experiment e6 was performed. Following the addition of 6 equivalents of NaDMM to 1 equivalent of $\text{Fe}(\text{CO})_2(\text{NO})_2$, the CO and NO bands of $\text{Fe}(\text{CO})_2(\text{NO})_2$ became barely detectable and $(\text{Fe}(\text{CO})(\text{NO})_2\text{DMM})^- \text{Na}^+$ was formed. With the introduction of CO , over a

period of several hours, the $\text{Fe}(\text{CO})_2(\text{NO})_2$ reappeared, thus indicating an equilibrium for reaction 2.3. To help confirm this, the addition of 1.5 equivalents of PPh_3 completely eliminated the $\text{Fe}(\text{CO})_2(\text{NO})_2$ and the $(\text{Fe}(\text{CO})(\text{NO})_2\text{DMM})^- \text{Na}^+$ peaks with the concomitant growth of the CO band of $\text{Fe}(\text{CO})(\text{PPh}_3)(\text{NO})_2$ at 1990cm^{-1} . Furthermore, the addition of 6.5 equivalents of α -methyl allyl acetate resulted in a very poor GC yield of crotyl-DMM at 9% and α -methyl allyl-DMM at 13%.

With

$(\text{Fe}(\text{CO})(\text{NO})_2\text{DMM})^- \text{Na}^+$ identified as one intermediate and $\text{Fe}(\text{CO})_3(\text{NO})^- \text{Na}^+$ as another in the reaction of $\text{Fe}(\text{CO})_2(\text{NO})_2$ with NaDMM , it must now be determined which species, $\text{Fe}(\text{CO})_3(\text{NO})^- \text{Na}^+$ or $(\text{Fe}(\text{CO})(\text{NO})_2\text{DMM})^- \text{Na}^+$ is the more likely to be responsible for the catalytic allylic alkylation reaction. Comparing the reaction times for both $\text{Fe}(\text{CO})_2(\text{NO})_2$ and $\text{Fe}(\text{CO})_3(\text{NO})^- \text{Na}^+$ reactions at equal Fe/allyl ratios, a very significant difference can be observed (see table 2.1, eF1 vs e7; eF2 vs e8). While the $\text{Fe}(\text{CO})_2(\text{NO})_2$ reactions took less than one hour to complete, the $\text{Fe}(\text{CO})_3(\text{NO})^- \text{Na}^+$ reactions took approximately 48h. Since the $\text{Fe}(\text{CO})_2(\text{NO})_2$ reaction was much faster than the $\text{Fe}(\text{CO})_3(\text{NO})^- \text{Na}^+$ reaction, it can be concluded that $(\text{Fe}(\text{CO})(\text{NO})_2\text{DMM})^- \text{Na}^+$ is the primary intermediate involved in the catalytic(s) cycle(s) with $\text{Fe}(\text{CO})_2(\text{NO})_2$ as its precursor. This system provided the first evidence of an interaction between the nucleophile and the metallic center in reactions involving iron nitrosyl complexes.

The fact that $(\text{Fe}(\text{CO})(\text{NO})_2\text{DMM})^- \text{Na}^+$ has been identified as the primary intermediate in the $\text{Fe}(\text{CO})_2(\text{NO})_2$ allylic alkylations does not exclude $\text{Fe}(\text{CO})_3(\text{NO})^- \text{Na}^+$ from being involved in a catalytic cycle. As previously stated, $\text{Fe}(\text{CO})_3(\text{NO})^- \text{Na}^+$ may react to form in-situ catalytically active nitrosyl carbonyl species. One such species is $\text{Fe}(\text{CO})_2(\text{NO})_2$. Furthermore, with the similar regioselectivities obtained

<i>Entry</i>	<i>Complex</i>	<i>Ln/Rm(a)</i>	<i>Stereochem</i>
eN1	syn($(\eta^3\text{-crotyl})\text{Fe}(\text{CO})_4$) ⁺	57, 43	E
eN2	anti($(\eta^3\text{-crotyl})\text{Fe}(\text{CO})_4$) ⁺	74, 26	Z
eN3	trans($\eta^2\text{-crotyl-OAc})\text{Fe}(\text{CO})_4$	40, 60	E
eN4	cis($\eta^2\text{-crotyl-OAc})\text{Fe}(\text{CO})_4$	71, 29	Z
eN5	Fe ₂ (CO) ₉ , trans-crotyl acetate	37, 63	E
eN6	Fe ₂ (CO) ₉ , cis-crotyl acetate	52, 48	Z

Table 2.3: Regio and stereoselectivity of nucleophilic addition or allylic alkylation with NaDMM obtained by Nicholas [31]. (a) Linear vs ramified.

for alkylations using either $\text{Fe}(\text{CO})_2(\text{NO})_2$ or $\text{Fe}(\text{CO})_3(\text{NO})^- \text{Na}^+$, the possibility of comparable reaction mechanisms remains.

The results of the $\text{Fe}(\text{CO})_2(\text{NO})_2$ catalytic allylic chloride alkylation reactions show conclusively that no π -allyl intermediate is implicated in the catalytic cycle. In all cases the alkylation occurred predominantly at the carbon where the leaving group was attached. For comparison, using $\text{PtCl}(\text{PPh}_3)(\eta^3\text{-crotyl})$, which proceeds via a η^3 -allyl complex in allylic alkylation reactions of α -methyl allyl acetate and crotyl acetate, the same mixture of alkylation product is obtained. This, whether or not one started with the linear or the ramified allylic isomer [38].

An interaction between the nucleophile and the metallic center has also been observed by Nicholas et al. [31] using iron carbonyl complexes. In table 2.3 can be found the results obtained by Nicholas for the catalytic reactions of cis- and trans-crotyl acetate with $\text{Fe}_2(\text{CO})_9$. The regioselectivity exhibited by the $\text{Fe}_2(\text{CO})_9$ catalyzed reactions is unexceptional when compared to the $\text{Fe}(\text{CO})_2(\text{NO})_2$ and $\text{Fe}(\text{CO})_3(\text{NO})^- \text{Na}^+$ catalyzed reaction. Also, the reaction times at room temperature, in THF, were from 3-5 days.

The intermediates postulated by Nicholas [31] are found in figure 2.4. Species B of figure 2.4 is not believed to be the true catalyst, but rather a catalyst precursor

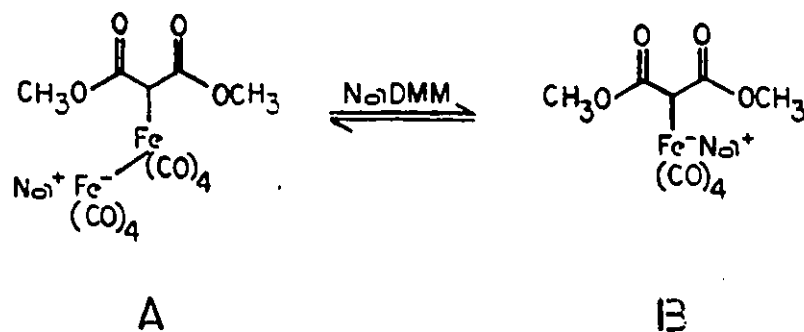


Figure 2.4: The $\text{Fe}_2(\text{CO})_9$ and NaDMM interaction intermediates postulated by Nicholas

since it reacted with crotyl acetates only in the presence of excess malonate ions.

Given that both the iron metal complexes $\text{Fe}(\text{CO})_2(\text{NO})_2$ and $\text{Fe}_2(\text{CO})_9$ interact with the nucleophile, and given the significant differences in the regioselectivities observed for the $\text{Fe}(\text{CO})_2(\text{NO})_2$ alkylations using allylic chlorides and the $\text{Fe}_2(\text{CO})_9$ alkylations using allylic acetates, a study of the $\text{Fe}(\text{CO})_2(\text{NO})_2$ allyl acetates alkylation is warranted.

2.1.3 The Allylic Acetates

The regioselectivity of the allylic acetate alkylation reactions varied from very good for the crotyl acetate reactions to poor for the α -phenyl allyl acetate reaction. These results are tabulated in tables 2.4 and 2.5. A comparison of the linear versus the ramified (e23 and e25 vs e16 and e26) allylic acetates showed that the linear allylic acetates gave a better overall yield and regioselectivity in alkylation product. When comparing the linear allylic acetates from least to most sterically hindered (crotyl acetate, cinamyl acetate, geranyl acetate), it is observed that the reactions times increase and that the overall yield decreases. This decrease in yield is such that, in the case of geranyl acetate the reaction would appear to be stoichiometric. In experiment e24, the addition of CO had no effect other than to increase the reaction

time.

As with the allylic chloride alkylations, the allylic acetate alkylations occurred predominantly at the carbon where the leaving group was attached, therefore demonstrating that $\text{Fe}(\text{CO})_2(\text{NO})_2$ forms active species in mediating allylic alkylations.

The refluxing of $\text{Fe}(\text{CO})_2(\text{NO})_2$ (0.1 eq.) and NaDMM (1.0 eq.) for 2h, followed by the addition of the crotyl acetate and a further 2h refluxing, gave very poor results (entry e21 compared to e20 and e22, table 2.4). This would seem to indicate that the catalytic species formed in the presence of $\text{Fe}(\text{CO})_2(\text{NO})_2$ and NaDMM was thermolabile and yielding inactive decomposition products.

In experiment e25 with cinamyl acetate as the allylic substrate, the only isolated product was cinamyl-DMM. However, for α -phenyl allyl acetate a product mixture of cinamyl-DMM / α -phenyl allyl-DMM in a ratio of 29:71 was obtained.

The results obtained for the geranyl acetate reactions e27 and e28 show that a significant amount of neryl-DMM was formed. This would indicate some loss of stereospecificity, and thus the possibility for isomerisation must be present at one point or another in the reaction mechanism.

To put the results of the $\text{Fe}(\text{CO})_2(\text{NO})_2$ catalyzed reactions in proper perspective, it is useful to compare these with other metal catalyzed alkylations. In table 2.6 are collected together regioselectivity data from the literature for crotyl acetate with DMM as nucleophile. Although the data for other metals with these basic reactants are rather limited, it appears that this substrate/nucleophile pairing generally leads to only poor to fair regioselectivity. The W and $\text{Fe}_2(\text{CO})_9$ catalyzed reactions show a modest selectivity for attack at the most substituted carbon or no selectivity at all for the present substrate/nucleophile combination. The $\text{Fe}(\text{CO})_2(\text{NO})_2$ and $\text{Fe}(\text{CO})_3(\text{NO})^- \text{Na}^+$ stand apart in promoting high selectivity for attack at the carbon

<i>Fe(CO)₂(NO)₂, α-methyl allyl acetate</i>							
<i>Rx</i>	<i>%M</i>	<i>Rx time</i>	<i>%Nu</i>	<i>GC %yeild</i>	<i>Regioselect</i>		<i>Comments</i>
					<i>Linear</i>	<i>Ramified</i>	
e10	9.5	3.5(1)	110	(56) ^a			
e11	10	3.5(1)	110	30	7	93	
e12	10	3.5(1)	110	33	3	97	
e13	10	(44)	110	16	6	94	
e14	10	9.5	110	27	4	96	
e15	10	2	110	39	3	97	
e16	20	6	100	67 (59) ^a	6	94	
eF3	30	14	100 ^b	79	5	95	Fe(CO) ₃ (NO) ⁻ Na ⁺
<i>Fe(CO)₂(NO)₂, crotyl acetate</i>							
e17	10	3.5(1)	110	(55) ^a			
e18	10	3.5(1)	110	56	95	5	
e19	10	3.5(1)	110	50	98	2	
e20	10.5	2	106	54	96	4	
e21	10.5	2+2	106	13	93	7	
e22	10.5	2	106	64	97	3	
e23	20	6	100	69 (50) ^a	88	12	
e24	10	40	100	60	90	10	CO
eF4	10	14	100 ^b	90	91	9	Fe(CO) ₃ (NO) ⁻ Na ⁺
eN5	10	(96)	200	90	37	63	Fe ₂ (CO) ₉ , trans-crotyl
eN6	10	(96)	200	90	52	48	Fe ₂ (CO) ₉ , cis-crotyl

Table 2.4: Results of Fe(CO)₂(NO)₂ mediated methyl-allyl acetate alkylation reactions. Reaction time in brackets is at room temperature. %M=Molar percent metal with respect to allyl substrate. %Nu=Molar percent NaDMM with respect to allyl substrate. (a) is isolated yield. (b) is NaDEM, sodium diethylmalonate. eF3 and eF4 are results obtained by Roustan et al. [30]. eN5 and eN6 are results obtained by Nicholas et al. [31].

<i>Fe(CO)₂(NO)₂, cinamyl acetate</i>							
<i>Rx</i>	<i>%M</i>	<i>Rx time</i>	<i>%Nu</i>	<i>GC %yield</i>	<i>%Regioselect</i>		<i>Comments</i>
					<i>Linear</i>	<i>Ramified</i>	
e25	20	<16	100	50 ^a	100		Fe(CO) ₃ (NO) ⁻ Na ⁺
eF5	10	14	100 ^b	91 ^a	100		
<i>Fe(CO)₂(NO)₂, α-phenyl allyl acetate</i>							
e26	20	<16	100	34 ^a	29	71	Fe(CO) ₃ (NO) ⁻ Na ⁺ Fe(CO) ₃ (NO) ⁻ Na ⁺
eF6	30	24	100 ^b	83 ^a	34	66	
eF7	30	24	100	81 ^a	23	77	
<i>Fe(CO)₂(NO)₂, geranyl acetate</i>							
e27	30	17	100	25	(2.5:1) ^c		
e28	33	(42)24	110	32	(3.2:1) ^c		

Table 2.5: Results of Fe(CO)₂(NO)₂ mediated allylic acetate alkylation reactions. Reaction time in brackets is at room temperature. %M=Molar percent metal with respect to allyl substrate. %Nu=Molar percent NaDMM with respect to allyl substrate. (a) Combined isolated yield of cinamyl-DMM and α-phenyl allyl-DMM. (b) NaDEM, sodium diethylmalonate. (c) geranyl-DMM to neryl-DMM ratio. eF5, eF6 and eF7 are results obtained by Roustan et al. [30].

<i>Substrate</i>	<i>Catalyst</i>	<i>ln/rm(a)</i>	<i>Reference</i>
crotyl acetate	Fe(CO) ₂ (NO) ₂	93,7	(b)
	Fe(CO) ₃ (NO) ⁻ Na ⁺	91,9	24
	Fe ₂ (CO) ₉	37,63	25
	W(CO) ₃ (CH ₃ CN)/bpy	24,76	5
crotyl chloride	Co(CO) ₃ NO	84,16	33

Table 2.6: Regioselectivity data for various metal mediated allylic alkylation reactions with crotyl acetate as the allylic substrate and DMM as the nucleophile. (a) Linear vs ramified. (b) This work.

which originally contained the leaving group.

The most interesting feature which emerges from the iron catalyzed allylic alkylation reactions is the conclusion that in the major product forming step(s), the catalytic reaction is not via an attack by nucleophile on either a $(\eta^2\text{-allyl X})\text{ML}_p$ or a $(\eta^3\text{-allyl})\text{ML}_n$ complex.

The significance of the above conclusion lies in the fact that $(\eta^3\text{-allyl})\text{ML}_n$ species are almost universally considered to be important intermediates in allylic alkylation reactions. In reality, however, rather little mechanistic information is available for these reactions. A few strictly comparable examples of a metal catalyzed process and its stoichiometric counterpart for Pd can be extracted from the literature [1,15,40], and these show similar or identical regioselectivities for reactions starting with either a crotylic substrate or its α -methylallyl isomer. Certainly, reports of allylic alkylation occurring with net retention of configuration at the substituted carbon (for Pd, Mo, and W) support a scheme wherein an $(\eta^3\text{-allyl})\text{ML}_n$ species is formed (with inversion at C) followed by external attack by Nu (also with inversion). On the other hand, alternate pathways involving two stereochemically retentive steps generally cannot be ruled out.

2.2 $\text{Fe}(\text{CO})_3(\text{NO})\text{-Na}^+$ Alkylation Reactions With Geranyl Acetate

Preliminary results from a study conducted by Roustan et al. [42], showed that geranyl acetate and neryl acetate undergo alkylation at the allylic position in the presence of $\text{Fe}(\text{CO})_3(\text{NO})\text{-Na}^+$ and either NaDMM or NaDEM. Furthermore, the study by Julia [17] showed that the geranyl acetate reactions were sensitive to the conditions in which the alkylation reactions occurred. Thus, further study of the

$\text{Fe}(\text{CO})_3(\text{NO})^- \text{Na}^+$, geranyl acetate reaction was needed.

Given that the reaction times, as monitored by IR were long and that such extended refluxing might lead to the decomposition of the substrates or to other reactions, a test reaction was monitored by both GC and IR. In reaction e29, (see figure 2.5) with $\text{Fe}(\text{CO})_3(\text{NO})^- \text{Na}^+$ (52%), NaDMM, and geranyl acetate , the IR's showed a steady decrease in NaDMM and no NaDMM after 41h. The $\text{Fe}(\text{CO})_3(\text{NO})^- \text{Na}^+$ IR peaks showed only a slight decrease. The GC graph showed a steady decrease in geranyl acetate and a steady increase in geranyl-DMM. From the graph, it can be seen that the reaction time for the completion of the reaction as monitored by GC was approximately 40h, which is in excellent agreement with the reaction time obtained by IR monitoring.

Three series of experiments were performed using three different methods of obtaining the $\text{Fe}(\text{CO})_3(\text{NO})^- \text{Na}^+$ anion. The first method, the deoxygenation of an NO_2^- ligand, was developed by Hieber [35]. It consists of reacting $\text{Fe}(\text{CO})_5$ with NaNO_2 to give $\text{Fe}(\text{CO})_3(\text{NO})^- \text{Na}^+$. The experimental conditions are, MeOH reflux in the presence of $\text{MeO}^- \text{Na}^+$, evaporation of the solvent , extraction with ether, addition of hexane, followed by partial evaporation of the solvent. The $\text{Fe}(\text{CO})_3(\text{NO})^- \text{Na}^+$, recovered as yellow crystals, contained one mole of MeOH per mole of $\text{Fe}(\text{CO})_3(\text{NO})^- \text{Na}^+$. The second method was developed by J.L. Roustan while this study was in progress. The reaction is a quantitative transfer of an NO ligand between $\text{Fe}(\text{CO})_2(\text{NO})_2$ and $\text{Na}_2\text{Fe}(\text{CO})_4 \cdot 1.5$ dioxane to give $\text{Fe}(\text{CO})_3(\text{NO})^- \text{Na}^+$. This reaction provides for an in-situ preparation of $\text{Fe}(\text{CO})_3(\text{NO})^- \text{Na}^+$ without MeOH. The third method was the use of samples of $\text{Fe}(\text{CO})_3(\text{NO})^- \text{Na}^+$ obtained in the solid state from the reaction by Roustan. There was one mole of 1,4-dioxane per mole of $\text{Fe}(\text{CO})_3(\text{NO})^- \text{Na}^+$.

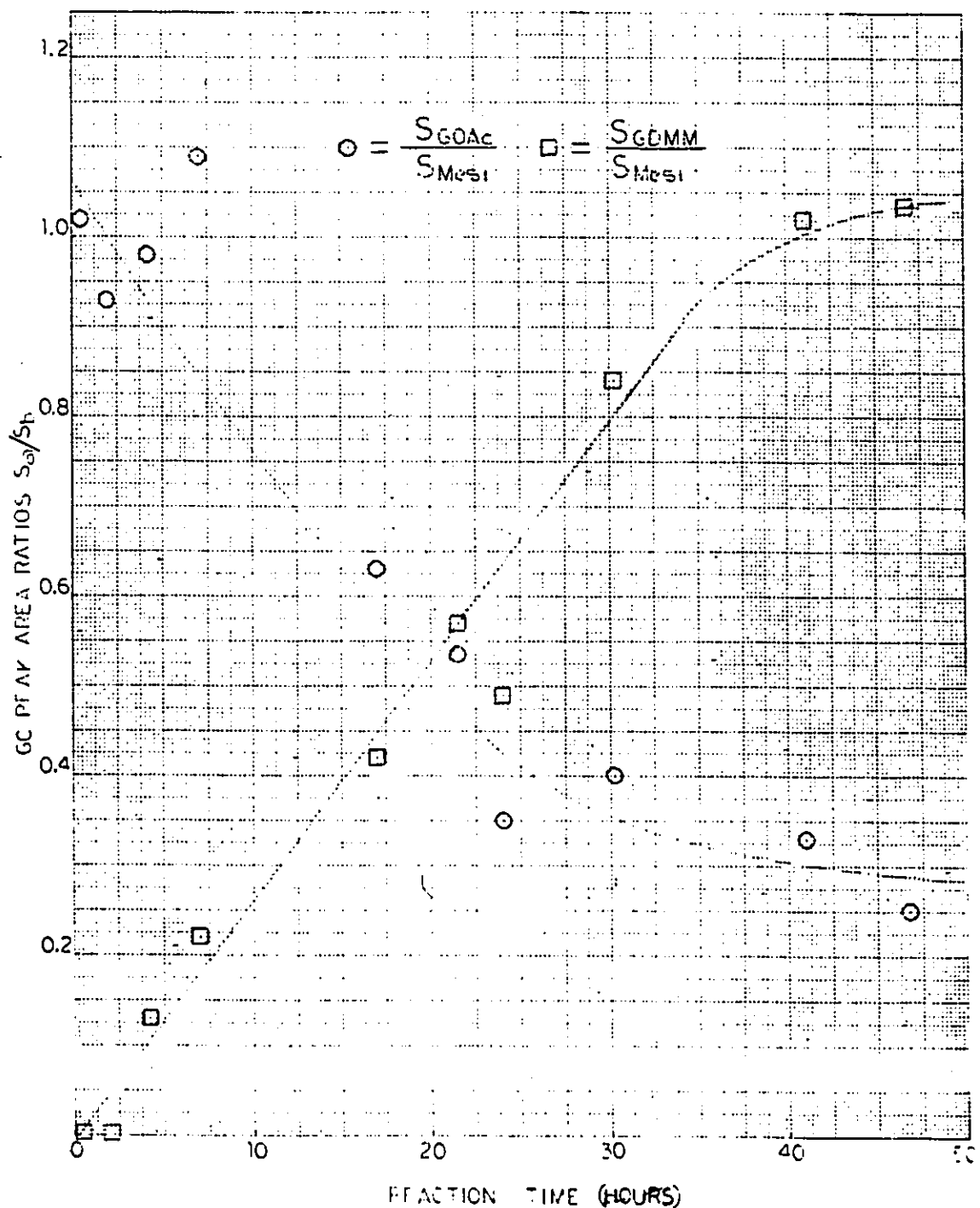


Figure 2.5: A plot of the product formation versus time with the substrates $\text{Fe}(\text{CO})_3(\text{NO})\text{-Na}^+$ (52%), NaDMM, and geranyl acetate. Where S_{GOAc} , S_{GDMM} , and S_{MeSi} are the GC integration peaks of geranyl acetate, geranyl dimethylmalonate, and mesitylene respectively.

<i>Fe(CO)₃(NO)⁻Na⁺·MeOH</i>							
<i>Rx</i>	<i>%M</i>	<i>Rx time</i>	<i>%NaDMM</i>	<i>%DMM</i>	<i>%yield</i>		<i>Comments</i>
					<i>GC</i>	<i>Wt</i>	
e31	55	40	100	100	54	47	MeOH
e32	49	20	110	100	76		
e33	30	40	110	100	62		
e34	50	40	110	100	65		
<i>Fe(CO)₃(NO)⁻Na⁺, in situ</i>							
e35	55	40	110	100		50	
e36	55	40	110	0		54	
<i>Fe(CO)₃(NO)⁻Na⁺·1,4-dioxane</i>							
e37	22	40	110	100	71	52	
e38	52	40	110	0	69	44	
e39	31.6	40	110	0	60		
e40	16	40	110	0	51		

Table 2.7: Results of $\text{Fe}(\text{CO})_3(\text{NO})^- \text{Na}^+$ mediated geranyl acetate alkylation reactions. Molar percent metal with respect to allyl substrate. % yield of alkylated product by GC and/or isolated.

In some of the reactions presented in table 2.7, no DMM was added to the reaction mixture. Under these conditions, apart from the monoalkylated products, formation of other products were detected by GC and notably products with retention times suggestive of the occurrence of a bisalkylation reaction.

One observes that in all reactions with geranyl acetate there is a partial loss of the stereochemistry of the double bond in the allylic position with respect to the leaving group (OAc), the geranyl-DMM / neryl-DMM ratio being approximately 3 ± 0.5 . This is the first case where the stereochemistry of the double bond is lost in reactions catalyzed by $\text{Fe}(\text{CO})_3\text{NO}^-$. The yields are in the 50-60% range regardless of the catalyst/substrate ratio used which vary from 16 to 55%. In reactions e34 (table 2.7), the addition of one equivalent of MeOH with respect to the catalyst had no significant effect. The IR spectra of the reaction mixture taken at the beginning and at the end of the reaction showed that there was only a decrease of 15% in the

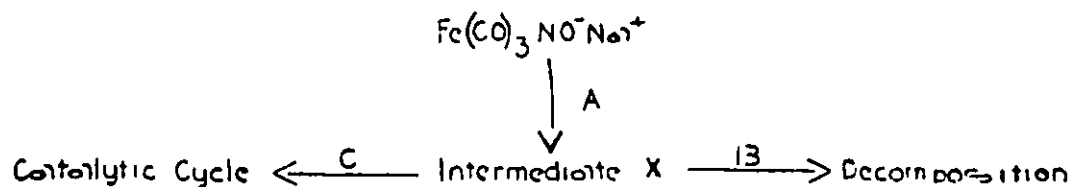


Figure 2.6: Postulated formation of an intermediate X from $\text{Fe(CO)}_3(\text{NO})^- \text{Na}^+$ transmittance of the CO bands of $\text{Fe(CO)}_3(\text{NO})^- \text{Na}^+$ in the 1980cm^{-1} region. In reactions e31, e35, and e38 even though the amount of alkylation product obtained is comparable to the quantity of catalyst used, it would be erroneous to conclude that $\text{Fe(CO)}_3(\text{NO})^- \text{Na}^+$ is a stoichiometric reactant. If it were so, it would have been totally consumed which it is not the case.

We conclude that $\text{Fe(CO)}_3(\text{NO})^- \text{Na}^+$ serves indeed as the precursor of a catalytic species X (see figure 2.6).

Of the reactions listed in table 2.7, e32 distinguishes itself because the reaction time was half that of the other reactions under apparently very similar conditions. There has been, in this case, an acceleration of the reaction which one can attribute to a higher concentration of intermediate X. This can be the result of either an increase in the rate of reaction A, a decrease in the rate of reaction B, or a combination of both of these.

In order to gather further evidence for the formation of an intermediate in the $\text{Fe(CO)}_3\text{NO}^-$ mediated reactions, geranyl acetate was replaced by allyl acetate thus allowing to run the alkylation reaction at room temperature. Under these conditions (e41), with the following reactants, $\text{Fe(CO)}_3(\text{NO})^- \text{Na}^+$ (25%), NaDMM, and allyl acetate, the reaction was monitored over time by both IR and GC. No excess of

DMM was added to allow the detection by IR of any intermediate with absorptions in the 1750-1700 cm^{-1} region.

In figure 2.7 are found four IR spectra taken during the course of the reaction. There are two notable spectral changes. The first is the decrease in the transmittance of the NaDMM absorption band at 1680 cm^{-1} from a situation where it was near 0 transmittance to a situation where it was barely detectable. The second is the way in which the CO bands of $\text{Fe}(\text{CO})_3(\text{NO})^- \text{Na}^+$ around 1980 cm^{-1} varied over time. In spectra S1 of figure 2.7, which is at $t=50\text{min}$ of the reaction, the 1980 cm^{-1} band has a profile which corresponds to a larger concentration in solvent separated ion pairs than in tight ion pairs, this in accord with observations made by Pannell [41] for $\text{Fe}(\text{CO})_3(\text{NO})^- \text{Na}^+$ in THF. At $t=2\text{h}$ (spectra T1) the profile of the 1980 cm^{-1} band has changed to one where the concentration of the tight ion pairs is greater than the solvent separated ion pairs with a concomitant decrease in the overall peak intensity. Then, with time, the profile of the 1980 cm^{-1} band reverts at $t=17\text{h}$ (spectra S2) to what it was at $t=50\text{min}$ (spectra S1). A spectra taken at $t=21\text{h}$ (spectra T2) shows that the tight ion pairs predominate once again over the solvent separated ion pairs.

In figure 2.8 is found a plot of the GC peak area ratio of product to internal standard (this being proportional to product formation) versus time. If one assumes that the GC values obtained at 17h and 21h are aberrations then one would draw the broken line curve indicated in figure 2.8. However, because of supporting IR data in figure 2.7, the GC value at 17h may not be dismissed as an aberration. Thus, the resulting curve in figure 2.8 is an S-curve as drawn by the solid line. This plot shows there was rapid product formation in the first 6h, flattening out in the next 11h, reacceleration of product formation in the following 4h and flattening out once more

after that.

This behavior is strongly suggestive of the formation of a species X which interacts strongly with the nitrosylic O atom of $\text{Fe}(\text{CO})_3\text{NO}^-$ to give a species Y, figure 2.9, which has the tight ion pair IR profile rather than the $\text{Fe}(\text{CO})_2(\text{NO})_2$ solvent separated ion pair IR profile. As long as the concentration of Y is sufficient the reaction will proceed. If Y is not reformed and there is decomposition then the reaction should stop. Thus, if there is no more Y the initial solvent separated ion pair IR profile of the beginning of the reaction should be observed. As is the case in figure 2.7 C. If Y is reformed for whatever reason when the substrate is still present, then the reaction would restart. As is observed in figure 2.8.

The rate acceleration of one alkylation reaction of geranyl acetate (e32) might then have been due to uncontrolled reaction conditions favouring product formation and/or the enhanced labilization of species X.

To answer whether or not X can be derived from $\text{Fe}(\text{CO})_2(\text{NO})_2$, itself derived from an in-situ decomposition of $\text{Fe}(\text{CO})_3(\text{NO})^- \text{Na}^+$, alkylation reactions of geranyl acetate with $\text{Fe}(\text{CO})_2(\text{NO})_2$ alone and/or in the presence of $\text{Fe}(\text{CO})_3(\text{NO})^- \text{Na}^+$ were studied in order to find conditions allowing for reaction times significantly smaller than those of 40h observed in most of the experiments involving this substrate.

2.3 Possible interactions between $\text{Fe}(\text{CO})_3(\text{NO})^- \text{Na}^+$ and $\text{Fe}(\text{CO})_2(\text{NO})_2$

Given that the decomposition of $\text{Fe}(\text{CO})_3(\text{NO})^- \text{Na}^+$ in reactions with geranyl acetate is of the order of 15%, then the concentration of species X in solution must surely be small. The addition of 30% $\text{Fe}(\text{CO})_2(\text{NO})_2$ in reaction e27 (table 2.8) ensures that if

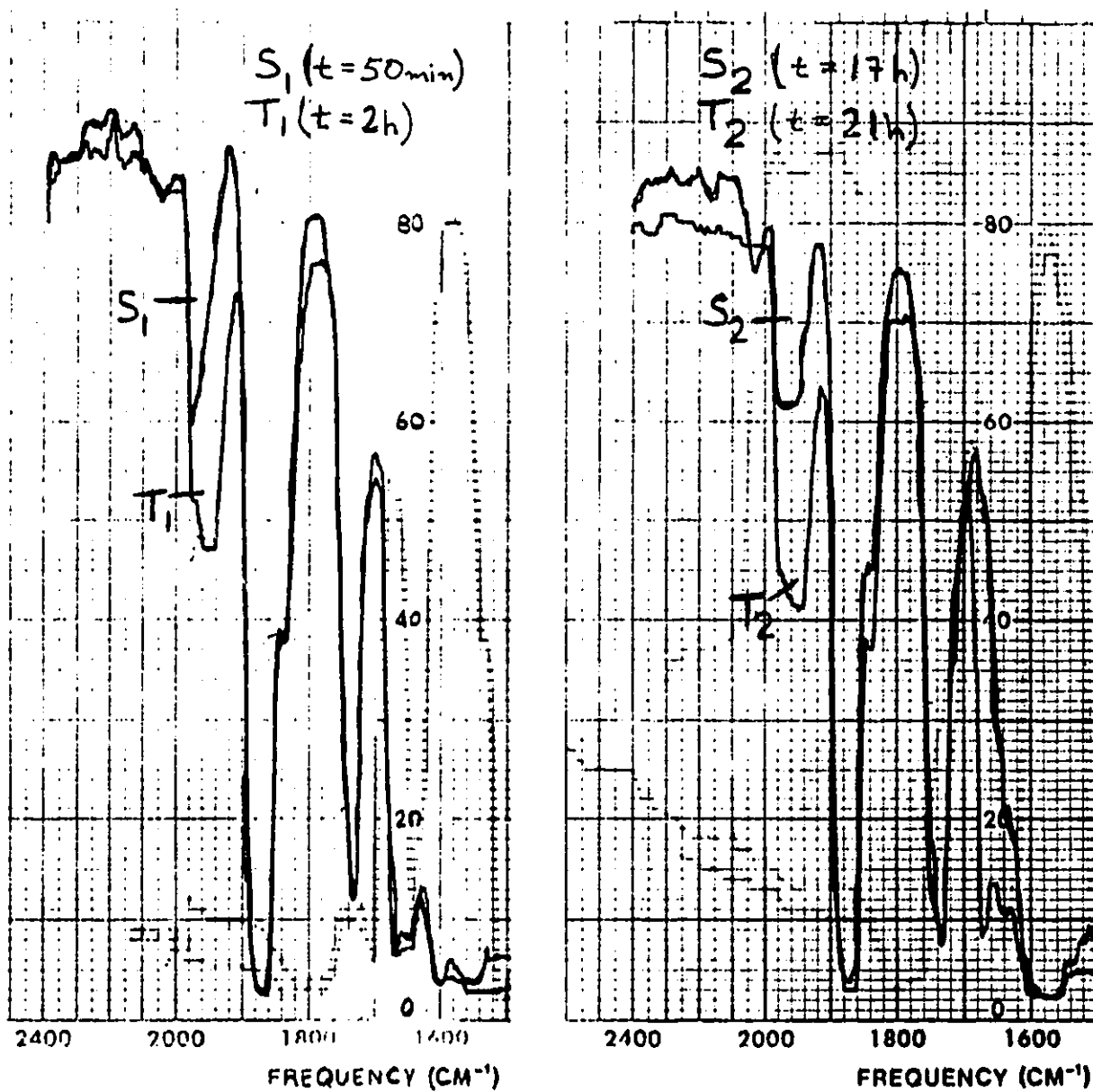


Figure 2.7: A series of IR spectra over time, of a reaction with the following reactants: $\text{Fe}(\text{CO})_3(\text{NO})^- \text{Na}^+$ (25%), NaDMM, and allyl acetate. S_1 ($t=50\text{min}$) and S_2 ($t=17\text{h}$) have a solvent separated ion pair profile for the 1980cm^{-1} band, whereas, T_1 ($t=2\text{h}$) and T_2 ($t=21\text{h}$) have a tight ion pair profile for the 1980cm^{-1} band.

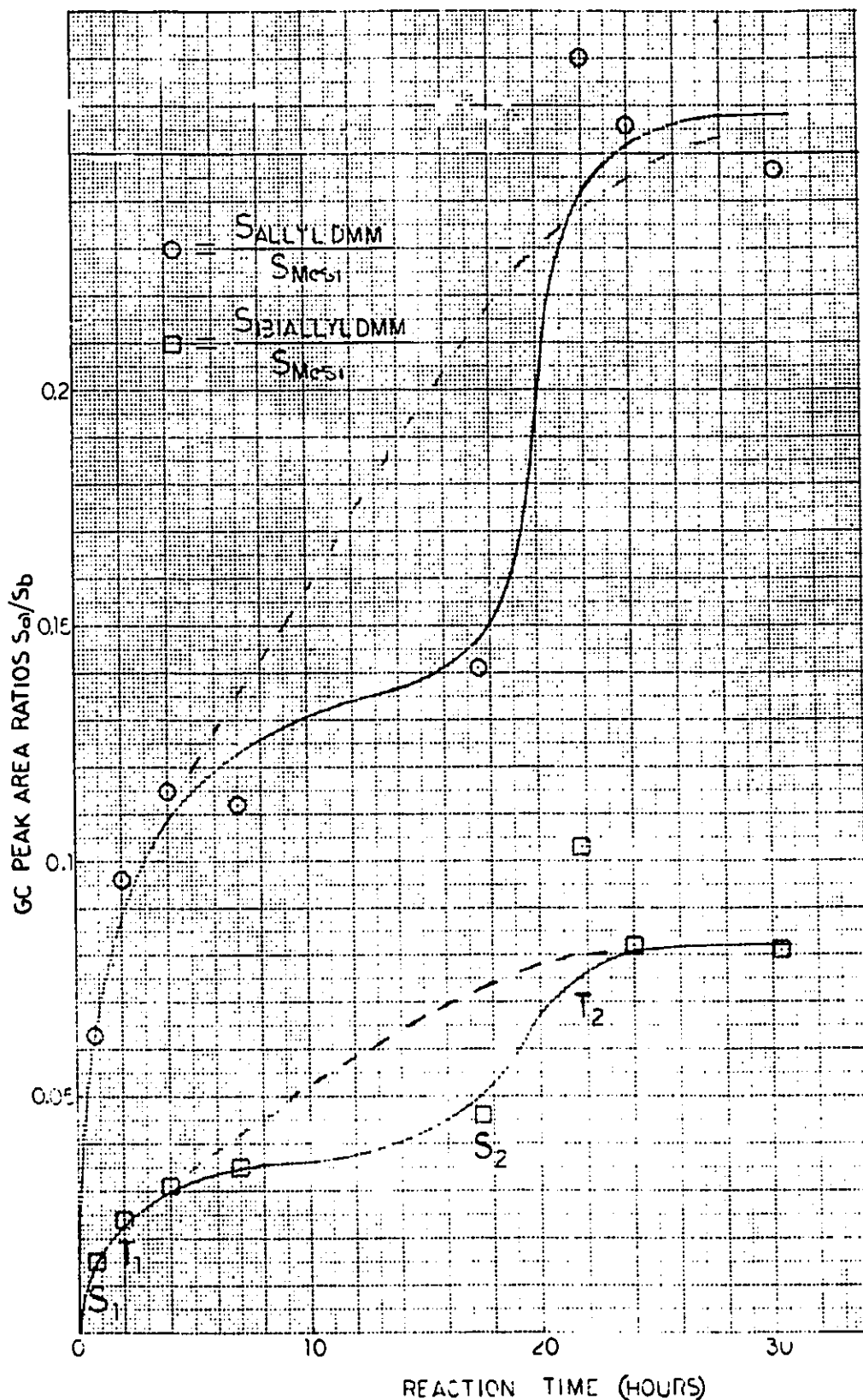


Figure 2.8: A plot of the GC peak area ratios S_a/S_b (where S_a is the GC peak area of the reaction product allyl-DMM or biallyl-DMM and S_b is the GC peak area of the internal standard mesitylene), which is proportional to product formation, versus time for a reaction with the substrates $\text{Fe}(\text{CO})_3(\text{NO})-\text{Na}^+$ (25%), NaDMM, and allyl acetate. The respective IR's of the reaction at points S_1 , T_1 , S_2 , and T_2 are found in figure 2.7.

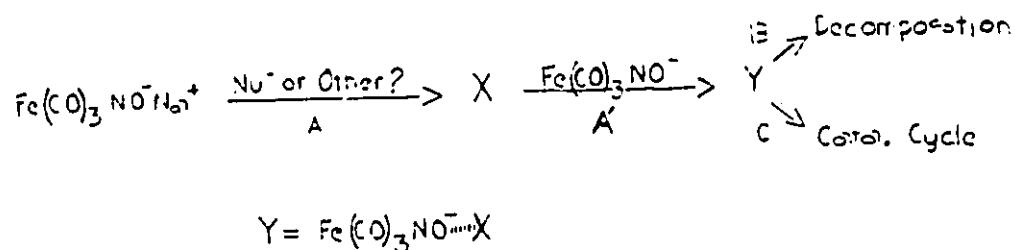


Figure 2.9: Postulated interaction of species X with $\text{Fe}(\text{CO})_3(\text{NO})^- \text{Na}^+$ to form species Y.

<i>Fe(CO)₂(NO)₂, Fe(CO)₃(NO)⁻Na⁺, geranyl acetate</i>					
<i>Rx</i>	<i>%M</i>	<i>Rx time</i>	<i>%Nu</i>	<i>GC %yield</i>	<i>Comments</i>
e27	30	17	100	25	Fe(CO) ₂ (NO) ₂
e28	33	(42)24	110	32	Fe(CO) ₂ (NO) ₂
e42	20	48	110	0	Fe(CO) ₂ (NO) ₂
	23	48	110	43	Fe(CO) ₃ (NO) ⁻ Na ⁺
e43	30	41	110	42	0.15 eq; 0.14 eq

Table 2.8: Results of $\text{Fe}(\text{CO})_2(\text{NO})_2$ and/or $\text{Fe}(\text{CO})_3(\text{NO})^- \text{Na}^+$, geranyl acetate reactions. Reaction time in brackets is at room temperature. %M=Molar percent metal with respect to allylic substrate. %Nu=Molar percent NaDMM with respect to allylic substrate. GC % yield of alkylated products with geranyl-DMM /neryl-DMM ratios equal to 3.0 ± 0.5 .

X is derived from $\text{Fe}(\text{CO})_2(\text{NO})_2$, its concentration would be much greater than in the $\text{Fe}(\text{CO})_3(\text{NO})^- \text{Na}^+$ reactions. Within 3.5h of the beginning of the reaction the $(\text{Fe}(\text{CO})(\text{NO})_2\text{DMM})^- \text{Na}^+$ was totally decomposed. Between 3.5h and 17h there was little change in the NaDMM 1680cm^{-1} IR band, so the reaction was stopped. The yield of 25% suggests the reaction is stoichiometric. Knowing that the reaction is thermolabile (e21, table 2.4), the reaction was repeated at room temperature (e28). With no changes observed in the IR after 42h, the reaction was refluxed for 24h. A similar result as above was obtained, thus the reaction is stoichiometric.

These results seem to indicate that X is not independent of $\text{Fe}(\text{CO})_3(\text{NO})^- \text{Na}^+$. There still remains the possibility that $\text{Fe}(\text{CO})_3(\text{NO})^- \text{Na}^+$ and $\text{Fe}(\text{CO})_2(\text{NO})_2$ and/or their product(s) of decomposition may interact to favour the formation of X.

The initial reaction conditions for experiment e42 (table 2.8) were such as to favor the decomposition of $\text{Fe}(\text{CO})_2(\text{NO})_2$ in the presence of geranyl acetate, therefore increasing the decomposition-geranyl acetate interactions rather than the $(\text{Fe}(\text{CO})(\text{NO})_2\text{DMM})^- \text{Na}^+$ -geranyl acetate interactions. NaDMM was added to a refluxing solution of $\text{Fe}(\text{CO})_2(\text{NO})_2$, geranyl acetate, and DMM, this over a period of one hour. Within 0.5h of having started the NaDMM addition, the $\text{Fe}(\text{CO})_2(\text{NO})_2$ bands were no longer detected in the IR spectrum. As well, the usual intermediate $(\text{Fe}(\text{CO})(\text{NO})_2\text{DMM})^- \text{Na}^+$ and $\text{Fe}(\text{CO})_3(\text{NO})^- \text{Na}^+$ peaks associated with the reaction of $\text{Fe}(\text{CO})_2(\text{NO})_2$ and NaDMM were not present. The solution was refluxed for 48h with no observable changes. Analysis of an aliquot by GC showed the presence of NaDMM as well as geranyl acetate but no products of alkylation or other unidentified species. Therefore, the products of decomposition of $\text{Fe}(\text{CO})_2(\text{NO})_2$ are not in themselves active species. Furthermore, in reactions e27 and e28, $(\text{Fe}(\text{CO})(\text{NO})_2\text{DMM})^- \text{Na}^+$ was truly the active species.

When 0.23 eq. of $\text{Fe}(\text{CO})_3(\text{NO})^- \text{Na}^+$ was added to the reaction mixture of e42 and refluxed a further 42h, alkylation did occur. The GC yield was 43%. The products of $\text{Fe}(\text{CO})_2(\text{NO})_2$ decomposition do not seem to have had any significant influence on the $\text{Fe}(\text{CO})_3(\text{NO})^- \text{Na}^+$ alkylation. Therefore, X is not a product of decomposition of $\text{Fe}(\text{CO})_2(\text{NO})_2$ in the absence of $\text{Fe}(\text{CO})_3(\text{NO})^- \text{Na}^+$.

Could the mixing of $\text{Fe}(\text{CO})_3(\text{NO})^- \text{Na}^+$ and $\text{Fe}(\text{CO})_2(\text{NO})_2$ provide products of decomposition which in this case would give better results? In experiment e43 (table 2.8), a solution containing the iron compounds $\text{Fe}(\text{CO})_2(\text{NO})_2$ (0.15 eq.) and $\text{Fe}(\text{CO})_3(\text{NO})^- \text{Na}^+$ (0.14 eq.), as well as, geranyl acetate, dimethylmalonate and NaDMM were brought to reflux. Within 5 minutes of adding NaDMM there were two bands in the carbonyl region, one at 1880cm^{-1} ($\text{Fe}(\text{CO})_3(\text{NO})^- \text{Na}^+$) and the other at 1980cm^{-1} . It could not be ascertained from the IR whether or not the 1980cm^{-1} band was due to $\text{Fe}(\text{CO})_3(\text{NO})^- \text{Na}^+$, $(\text{Fe}(\text{CO})(\text{NO})_2\text{DMM})^- \text{Na}^+$, or a combination of these. The GC yield was 42%. This result is no better than that obtained for e42. Therefore, it must be concluded that species X is not derived from $\text{Fe}(\text{CO})_2(\text{NO})_2$ directly or indirectly.

The search for an identifiable catalytic intermediate in allylic alkylation reactions involving $\text{Fe}(\text{CO})_3(\text{NO})^- \text{Na}^+$ is inconclusive.

2.4 Conclusion

In this work it has been shown that $\text{Fe}(\text{CO})_2(\text{NO})_2$ mediated allylic alkylation reactions proceed via an intermediate which is neither an η^3 -allyliron complex nor an η^2 -allyliron complex. Rather, $(\text{Fe}(\text{CO})(\text{NO})_2\text{DMM})^- \text{Na}^+$ has been identified as the catalytic intermediate. This provides the first evidence of an interaction between the nucleophile and the metallic center in reactions involving iron nitrosyl complexes.

The study of the $\text{Fe}(\text{CO})_3(\text{NO})^- \text{Na}^+$, geranyl acetate , and NaDMM system was studied in order to elucidate the catalytically active species. Although it was determined that $\text{Fe}(\text{CO})_3(\text{NO})^- \text{Na}^+$ served as the precursor of a catalytic species X, the nature of X remains unknown.

Chapter 3

Experimental Section

3.1 General

Unless otherwise stated, all operations were carried out under an argon pure atmosphere using standard vacuum line and Schlenk techniques. Glassware was cleaned using chromic acid, distilled water and reagent grade acetone. Prior to use, glassware was fitted together, pumped under vacuum and dried using a high temperature blow dryer.

^1H and ^{13}C NMR spectra were recorded on a Varian XL-300 spectrometer. All NMR chemical shifts were reported relative to tetramethylsilane. Infrared spectra of the solution with the appropriate solvent in the reference cell were recorded on a Perkin-Elmer 283 spectrometer, calibrated with a polystyrene film. Mass spectra were determined on a VG analytical 7070E GC/mass spectrometer. Analytical GC were carried out on a Varian Vista 6000 using a 5ft x 1/8 in. OV 17 packed column and a flame ionized detector. Preparative column chromatography was conducted on silica gel (Fisher) using a hexane / ethyl acetate mixture as eluent. Thin layer preparative chromatography was conducted on either glass plates loaded with silica gel 1mm thick (Kieselgel) or prepared silica gel plates purchased from Analtech Inc..

Reagent grade tetrahydrofuran (THF) (Fisher) was freshly distilled over sodium

and benzophenone (Baker) under nitrogen (high dry). Argon was then bubbled through the THF for at least 0.5h. Reagent grade dichloromethane (CH_2Cl_2)(Fisher) was freshly distilled under nitrogen from P_2O_5 (Baker). The NMR solvent CDCl_3 (aldrich) was dried over molecular sieves. Anhydrous ether (Mallinkrodt) was used as received and stored under an argon atmosphere.

3.2 Preparation of the Dimethyl Malonate Anion, NaDMM

In a Schlenk flask two equivalents of sodium hydride were added (NaH ; 50% dispersion in oil). 2 x 15 ml of anhydrous ether was used to wash out the oil, each fraction being pumped dry using a canula with a filter paper attached. The sodium hydride was further dried under vacuum. The flask containing the dry sodium hydride was placed under an argon atmosphere and 50 ml of THF was added. While stirring, in order to get a suspension of NaH , one equivalent of dimethyl malonate, DMM (Aldrich), was added slowly in order to control the rate of production of hydrogen. After the dimethyl malonate addition was complete the solution was stirred for another 2h and then left for 15h under argon, in order to decant the excess NaH . This provided a standard solution of the dimethyl malonate (NaDMM) anion.

3.3 Preparation of the Acetates

3.3.1 crotyl acetate

In a 250 ml round bottom flask fitted with a reflux condenser, a pressure equalized dropping funnel and an argon outlet was added 12.8 ml (0.15 moles) of 2-buten-1-ol (Aldrich) and 44ml (0.54 moles) of pyridine (Fisher). Acetic anhydride (Baker) 44 ml (0.54 moles) was slowly added to the stirring mixture. The addition completed,

the reaction mixture was refluxed (130-140°C) for approximately 4h. The mixture was dissolved in 200 ml of ether and washed, first with 4 x 200 ml of a saturated aqueous NaHCO₃ solution, second with 4 x 200 ml of an aqueous 2.5% HCl solution, and finally with 4 x 200 ml of a saturated brine (NaCl) solution. The final ethereal phase was checked with pH paper (neutral) and dried with MgSO₄ (Baker). The dried solution was filtered and the ether evaporated on a rotary evaporator. The remaining organic phase was distilled (122 - 134°C) yielding 11.1 g (65%) of crotyl acetate . Characterization was accomplished by ¹H NMR.

¹H: 1.70(D;3H), 2.05(S;3H), 4.40(D;2H), 5.60(M;2H).

3.3.2 α-methyl allyl acetate

Using the same experimental procedure as for crotyl acetate , 11.0 ml (0.139 moles) of 3-buten-2-ol (Aldrich) was added to 40.0 ml (0.501 moles) of pyridine followed by the slow addition of 40.4 ml (0.429 moles) of acetic anhydride. The mixture was refluxed for 4h. After work-up (see above section) the product was distilled (104-112°C) at atmospheric pressure yielding 9.5g (60%) of α-methyl allyl acetate . Characterization was accomplished by ¹H NMR.

¹H: 1.30(D;3H), 2.05(S;3H), 5.00(M;2H), 5.20(M;1H), 5.60(M;1H).

3.3.3 geranyl acetate

Using the same preparatory and work-up procedure as for crotyl acetate , 9.0 ml (0.052 moles) of geraniol (Aldrich) was added to 15.0 ml (0.188 moles) of pyridine. Acetic anhydride, 16 ml (0.177 moles), was added to the mixture. After refluxing, work-up and reduced pressure distillation (155°C , 39.3 mm), 8.2g (77%) of geranyl acetate was isolated and characterized by ¹H NMR.

3.3.4 neryl acetate

Using the same preparatory and work-up procedure as for crotyl acetate , 9.0 ml (0.052 moles) of nerol (Aldrich) was added to 15.0 ml (0.188 moles) of pyridine. To this was added 16.7 ml (0.177 moles) of acetic anhydride. After refluxing and work-up the crude product was distilled under reduced pressure (155-157°C , 38 mmHg) and 8.4g (82%) of neryl acetate was obtained and characterized by ¹H NMR.

3.3.5 cinamyl acetate

Using the same experimental procedure as in the preparation of crotyl acetate , 10 g (0.075 moles) of 3-phenyl-2-propenol (Aldrich) was added to 22.0 ml (0.270 moles) of pyridine. This was followed by the dropwise addition, with stirring, of 21.8 ml (0.231 moles) of acetic anhydride and refluxing for 4h. The crude product was distilled at reduced pressure yielding 8.9 g (67%) of cinamyl acetate . The characterization was accomplished by ¹H NMR and MS-GC.

¹H: 2.10(S;3H), 4.75(D;2H), 6.40(M;2H), 7.30(M;5H).

MS-GC: RT = 7:56, *M*⁺ = 176.0, Base = 43.1

3.3.6 α-phenyl allyl acetate

The α-phenyl allyl acetate was available in the lab from a previous study. The purity of the clear liquid was verified by GC and characterized by ¹H NMR.

¹H: 1.93(S;3H), 5.11(M;2H), 5.84(M;1H), 6.10(M;1H), 7.17(M;5H).

3.4 Preparation of Iron Compounds

3.4.1 Iron Dinitrosyl Dicarbonyl, $\text{Fe}(\text{CO})_2(\text{NO})_2$

Iron dinitrosyl dicarbonyl was prepared according to the following method [34]. A 300 ml three neck round bottom flask fitted with a pressure equalized dropping funnel, N_2 inlet and a cold gas trap was flushed with nitrogen. This was followed by addition of 160 ml of H_2O (N_2 saturated), 20.0 g (0.500 mole) of NaOH, 12.0 g (0.174 mole) of NaNO_2 , and 10.0 ml (14.6 g, 0.0746 mole) of iron pentacarbonyl respectively. The mixture was refluxed at 90 - 100°C for 3h. The vapours condensing were colourless. A 1:1 solution of glacial acetic acid in water (28.63 ml of glacial acetic acid) was added dropwise until yellow-brown fumes of $\text{Fe}(\text{CO})_2(\text{NO})_2$ began to form. The acid/ H_2O addition was discontinued and pure glacial acetic acid was added. During the addition of the 1:1 solution the reaction mixture was maintained at 42 - 45°C. The N_2 flow was increased in order to drive all the $\text{Fe}(\text{CO})_2(\text{NO})_2$ formed into a cold trap at 0°C. The red product was distilled into a second trap containing phosphorus pentoxide for final drying. The dried product was then transferred to a third trap by vacuum distillation. The yield of $\text{Fe}(\text{CO})_2(\text{NO})_2$ was 4.78g, 37% (3.23 ml., 0.0278 mole).

IR data: ν CO's, 2080 cm^{-1} (s), 2025 cm^{-1} (vs); ν NO's, 1810 cm^{-1} (s), 1760 cm^{-1} (vs), in CH_2Cl_2 .

3.4.2 Sodium Tricarbonylnitrosyl Iron Methanolate; $\text{Fe}(\text{CO})_3\text{NO}^-\text{Na}^+\cdot\text{CH}_3\text{OH}$

The published procedure of Hiebner et al.[35] was followed by reacting $\text{Fe}(\text{CO})_5$ with Na^+NO_2^- in absolute methanol in the presence of $\text{CH}_3\text{O}^-\text{Na}^+$ [36]. After completion of the reaction, the solvent was removed under reduced pressure and the solid residue dried under vacuum for at least 24h at room temperature. $\text{Fe}(\text{CO})_3(\text{NO})^-\text{Na}^+$ was

extracted with ether and the filtered solution concentrated under vacuum at 0°C until a few crystals appeared. Further cooling to -10°C with the addition of hexane and efficient stirring afforded most of the compound in the solid state. The solid was separated from the slightly colored solution, washed with hexane and benzene, and dried under vacuum (3h). The solid retained approximately 1 mol of methanol/mol of anion. It was sensitive to water, oxygen, and light and was stored under argon at 0°C. Over several months, the yellow color turned slightly green, presumably reflecting some oxidation. IR data: THF-tight ion pairs ν CO's 1990 cm^{-1} (s), 1890 cm^{-1} (s), ν NO 1615 cm^{-1} (s); loose ion pairs ν CO's 1977 cm^{-1} (s), 1873 cm^{-1} (sh), ν NO 1648 cm^{-1} .[37]

3.4.3 Sodium Tricarbonylnitrosyl Iron-1,4 Dioxanolate ; $\text{Fe}(\text{CO})_3(\text{NO})^- \text{Na}^+ \cdot 1,4\text{-dioxane}$

Under continuous argon flow, 0.497g (1.44 mmol) of $\text{Fe}(\text{CO})_4^{2-} 2\text{Na}^+ \cdot 1.5$ dioxane was transferred from a storage Schlenk to a reaction vessel. The $\text{Fe}(\text{CO})_4^{2-} 2\text{Na}^+ \cdot 1.5$ dioxane (insoluble in THF) was stirred for 10 minutes. To this was added 60 ml of THF and 0.217g (1.27 mmol) of $\text{Fe}(\text{CO})_2(\text{NO})_2$. The IR of the solution had the typical $\text{Fe}(\text{CO})_3(\text{NO})^- \text{Na}^+$ IR peaks but no $\text{Fe}(\text{CO})_2(\text{NO})_2$ peaks were observed. The $\text{Fe}(\text{CO})_3(\text{NO})^- \text{Na}^+$ was recrystallized from ether and dioxane. The yellow crystals contained one mole of 1,4-dioxane per mole of $\text{Fe}(\text{CO})_3(\text{NO})^- \text{Na}^+$.

3.5 GC Calibration Curves

3.5.1 crotyl-DMM

A 0.157M standard solution of the external reference mesitylene (Eastman) was prepared by adding 0.1885 g (0.57 mmol) of mesitylene to a 10 ml volumetric flask

<i>crotyl-DMM (1)</i>							
S_{C-DMM}/S_{mes}	0.066	0.153	0.249	0.358	0.445	0.673	1.405
N_{C-DMM}/N_{mes}	0.161	0.322	0.482	0.643	0.858	1.287	2.573
<i>Slope</i>	1.814						
<i>Intercept</i>	0.036						
<i>Correlation</i>	0.999						
<i>RT</i>	8.35 (C-DMM)			4.65 (mesitylene)			
<i>crotyl-DMM (2)</i>							
S_{C-DMM}/S_{mes}	0.379	0.178	0.133	0.764	1.50		
N_{C-DMM}/N_{mes}	0.69	0.29	0.23	1.37	2.59		
<i>Slope</i>	1.74						
<i>Intercept</i>	0.01						
<i>Correlation</i>	0.999						
<i>RT</i>	11.90 (C-DMM)			6.60 (mesitylene)			

Table 3.1: crotyl-DMM gas chromatograph calibration curves where S_{C-DMM}/S_{mes} is the crotyl-DMM to mesitylene GC peak area ratio, N_{C-DMM}/N_{mes} is the molar ratios, and RT the retention time.

and bringing to volume with CH_2Cl_2 . A 0.101M crotyl-DMM standard solution was made by adding 0.1885 g (1.01mmol) of crotyl-DMM to a 10 ml volumetric flask and bringing it to volume with CH_2Cl_2 (see table 3.1). Different samples with varying mes/crotyl-DMM ratios were made up. From each sample a 1 μl aliquoit was injected into the GC. The peak area ratios obtained were plotted against the known molar ratios of each sample.

3.5.2 α -methyl allyl-DMM

A standard 0.301 M solution of a mixture of crotyl-DMM / α -methyl allyl-DMM was prepared by adding 0.5603 g of a crotyl-DMM / α -methyl allyl-DMM mixture of unknown mole ratio to a 10 ml volumetric flask and bringing to volume with CH_2Cl_2 . A standard 0.166 M mesitylene solution was prepared by adding 0.200g of mesitylene to a 10.0 ml volumetric flask and brought to volume with CH_2Cl_2 . Different samples

<i>α-methyl allyl-DMM</i>						
$S_{ama-DMM}/S_{mesi}$	0.538	0.414	0.311	0.213	0.108	0.168
$N_{ama-DMM}/N_{mesi}$	0.747	0.620	0.452	0.283	0.139	0.247
<i>Slope</i>	1.443					
<i>Intércept</i>	-0.0068					
<i>Correlation</i>	0.996					
<i>RT</i>	11.90 (crotyl-DMM)			6.60 (mesitylene)		

Table 3.2: α -methyl allyl-DMM gas chromatograph calibration curves where, $S_{ama-DMM}/S_{mesi}$ is the α -methyl allyl-DMM to mesitylene GC peak area ratios, $N_{ama-DMM}/N_{mesi}$ is the molar ratio, and RT the retention time.

with varying mesi/mixture ratios were prepared and $1\mu\text{l}$ from each sample was injected into the GC. The peak area ratios for crotyl-DMM /mesi were obtained from the chromatograms and were compared with the previously constructed crotyl-DMM calibration curve (3.1) to obtain the respective number of moles of crotyl-DMM . With the number of moles of the mixture known to be present in each sample and having determined the number of moles of crotyl-DMM present, it was possible to calculate the number of moles of α -methyl allyl-DMM . ($N_{mix} - N_{crotyl} = N_{\alpha\text{-methyl}}$) It was then possible to calculate the α -methyl allyl-DMM /methyl mole ratios and to plot them against their respective GC area ratios. (See table 3.2.)

3.5.3 geranyl-DMM

Two calibration curves for geranyl-DMM were constructed, one for samples run under GC conditions which gave retention times (RT) of 16.7 min. for geranyl-DMM , 16.2 min. for neryl-DMM and 4.30 min. for mesitylene. The second curve was for GC conditions giving RTs of 18.6, 18.2, and 6.7 respectively. Each sample was prepared by weighing in a vial x grams of geranyl-DMM and x grams of mesitylene and adding 2 ml of CH_2Cl_2 . An aliquoit of this was injected into the GC and the peak area ratios obtained were plotted against the known molar ratios of each sample. It should be

geranyl-DMM (1)							
S_{G-DMM}/S_{mes}	0	0.953	2.17	0.533	1.27	2.40	
N_{G-DMM}/N_{mes}	0	0.72	1.78	0.42	0.868	1.87	
Slope	0.805						
Intercept	-0.035						
Correlation	0.996						
RT	16.67; 16.19 (G-DMM)				4.30 (mesitylene)		
geranyl-DMM (2)							
S_{G-DMM}/S_{mes}	0	1.54	1.22	0.633	0.949	0.237	2.65
N_{G-DMM}/N_{mes}	0	1.8	1.4	0.59	1.1	0.27	2.8
Slope	1.08						
Intercept	0.014						
Correlation	0.996						
RT	18.60; 18.20 (G-DMM)				6.70 (mesitylene)		

Table 3.3: geranyl-DMM gas chromatograph calibration curves where, S_{G-DMM}/S_{mes} is the geranyl-DMM to mesitylene GC peak area ratio, N_{g-DMM}/N_{mes} is the molar ratio, and RT the retention time.

noted that pure geranyl-DMM was never isolated. Thus, the geranyl-DMM used for the calibration curves was a mixture of geranyl-DMM and neryl-DMM in a ratio of 5:1 for the first plot and 3:1 for the second plot. (See table 3.3.)

3.6 $Fe(CO)_2(NO)_2$ Alkylation Reactions

3.6.1 General Experimental for Alkylation Reactions

The typical reaction conditions for the alkylation reactions were as follows: In a Schlenk tube under argon atmosphere, $Fe(CO)_2(NO)_2$ was dissolved in freshly distilled, argon saturated THF. The molar ratio of iron with respect to the allylic substrate varied from 10 to 100%. To this clear red solution was added one equivalent (with respect to the allylic substrate) of the sodium dimethyl malonate anion (NaDMM), and the optional addition of dimethyl malonate (DMM). This was followed by the addition of one equivalent of the allylic substrate. With the chloro

substituted allylic substrates, the mixture was stirred at room temperature. For the allylic acetates, the solution was at THF reflux. The reaction time were varied from 0.5h to 72h. Some of the reactions were monitored by observing both the disappearance and appearance of the starting materials and products respectively by IR and TLC. The work-ups were carried out by quenching the reaction mixture with approximately one equivalent of trifluoroacetic acid CF_3COOH (MCB or J.T.Baker) and then removing the solvent under vacuum at 25°C . The residue was dissolved in either an ether/water mixture or a methylene chloride /1% aqueous HCl mixture. The organic phase was dried over MgSO_4 and filtered. The solvent was removed at room temperature under vacuum. To the crude product mixture was added a known quantity of mesitylene, used as the internal standard for the GC yields. A gas chromatogram was taken of this crude product and the GC yields were calculated using previously established standard curves. Some of the crude product mixtures were further purified by column chromatography, preparative thin layer chromatography, or by reduced pressure distillation. The hexane/ethylacetate eluant ratio for the column was 10:1, whereas for the TLC separations one elution with hexane was followed by one elution of 20:1 hexane/ethylacetate. The isolated products were verified for purity by GC and characterized by either ^1H NMR, ^{13}C NMR, GC-MS, or a combination of these.

3.6.2 Alkylation of Allylic Chlorides

Reaction e1

To a solution of 20 ml of THF containing 0.8 mmol (1 ml @ 0.8M) of $\text{Fe}(\text{CO})_2(\text{NO})_2$ was added 8.0 mmol (40 ml @ 0.20M) of NaDMM. This solution was stirred for 15 minutes before adding 8.0 mmol (0.8 ml) of 3-chloro-1-butene

<i>crotyl-DMM</i>	
1H	1.56(M;3H), 2.51(M;2H), 3.35(S;1H), 3.68(S;6H), 5.33(M;1H), 5.52(M;1H)
^{13}C	17.83, 31.85, 51.89, 52.36, 126.25, 128.45, 169.37.
<i>α-methyl allyl-DMM</i>	
1H	1.02(D;3H), 2.90(M;1H), 3.26(D;1H), 3.65(S;6H), 5.02(M;2H), 5.71(M;1H)
^{13}C	17.82(17.85), 38.04, 52.21(52.30), 57.47, 115.44, 139.60, 168.55(168.61)
<i>cinamyl-DMM</i>	
1H	2.77(M;2H), 3.49(T;1H), 3.68(S;6H), 6.10(M;1H), 6.43(M;1H), 7.24(M;5H)
<i>MS-GC</i>	RT = 9:48, M^+ = 247.9, Base = 129.0; RT = 10:20, M^+ = 247.9, Base = 129.0
<i>α-phenyl allyl-DMM</i>	
1H	3.44(S;3H), 3.70(S;3H), 3.84(M;1H), 4.08(M;1H), 5.08(M;2H), 5.96(M;1H), 7.22(M;5H)
<i>MS-GC</i>	RT = 8:26, M^+ = 248.0, Base = 189.0; RT = 8:28, M^+ 248.0, Base 189.0
<i>geranyl-DMM</i>	
1H	1.55(S;3H), 1.59(S;3H), 1.64(M;3H), 1.97(T;2H), 2.01(M;2H), 2.59(T;2H), 3.35(T;1H), 3.68(S;6H), 5.02(M;2H)

Table 3.4: NMR data of the products of the various allylic alkylation reactions.

(Aldrich) and stirred for a further 13h at room temperature under a continuous argon flow. The reaction was monitored by IR. The solution mixture was worked-up by adding 8.0 mmol (0.7 ml) of CF_3COOH , extraction using Et_2O and H_2O , drying with MgSO_4 , and addition of 3.6 mmol (0.4325g) of mesitylene. The GC yields were α -methyl allyl-DMM at 38%, crotyl-DMM at 22%, and bisalkylation at ~15%.

Reaction e2

Using the same reaction and work-up procedure as in reaction e1 and using the following quantities of reagents, GC yields of 8% for α -methyl allyl-DMM, 40% for crotyl-DMM and ~20% for bisalkylation were obtained: THF, 20 ml; NaDMM, 8mmol (40 ml @ 0.20M); $\text{Fe}(\text{CO})_2(\text{NO})_2$, 0.8 mmol (1ml @ 0.8M); crotyl chloride, 10.0 mmol (1.0 ml) (Aldrich); mesitylene, 3.6 mmol (0.432g); CF_3COOH , 8.0 mmol (0.7ml).

Reaction e3

To a solution of 20 ml THF containing 0.8 mmol (1 ml @ 0.8M) of $\text{Fe}(\text{CO})_2(\text{NO})_2$ and 8.0 mmol (40 ml @ 0.20M) was added carbon monoxide by bubbling the gas through the solution. 25 minutes later 8.0 mmol (0.8 ml) of 3-chloro-1-butene was added and the solution mixture stirred at room temperature and under a continuous flow of CO for 13h. The solution was monitored by IR. The usual CF_3COOH (8 mmol, 0.7 ml) Et_2O / H_2O work-up was used. With 3.6 mmol (0.432g) of mesitylene added to the product mixture, the following GC yields were obtained: α -methyl allyl-DMM, 33%; crotyl-DMM, 22%; bisalkylation, ~15%.

Reaction e4

Using the same experimental and work-up procedure as in reaction e3 and the following quantities of reagents, GC yields of 7% for α -methyl allyl-DMM, 50% for crotyl-DMM and ~20% for bisalkylation were obtained: $\text{Fe}(\text{CO})_2(\text{NO})_2$, 0.8 mmol

(1ml @ 0.8M); NaDMM, 8.0 mmol(40 ml @ 0.20M); crotyl chloride , 10.0 mmol (1.0 ml); CF₃COOH, 8.0 mmol (0.7 ml); mesitylene, 3.6 mmol (0.432g).

Reaction e5

To a 50 ml solution of THF with bubbling CO was added 2 ml @ 0.43M (0.86 mmol) of NaDMM in THF, 0.10 ml (0.86 mmol) of Fe(CO)₂(NO)₂, and 5 ml of THF. The solution was stirred at room temperature for 2.5h after which 0.09 ml (0.9 mmol) of 3-chloro-1-butene was added. This solution mixture was stirred at room temperature for 1.5h followed by the addition of 4 ml @ 0.43M (1.72 mmol) of NaDMM in THF and 4 ml of THF. Half an hour later 0.16 ml (1.6 mmol) of 3-chloro-1-butene was added and the solution was left stirring at room temperature for 21.5h at which time 20 ml @ 0.43M (8.6 mmol) of NaDMM in THF and 10 ml THF were added. Half an hour later 0.9 ml (9.0 mmol) of 3-chloro-1-butene was added and the solution mixture was left stirring under static CO for 3 days. It was finally heated 3.5h at THF reflux. The solution was worked-up by first adding CF₃COOH, evaporating the solvent, extracting with an Et₂O / H₂O mixture, redissolving the crude products in Et₂O, and adding 0.4325g (3.6 mmol) of mesitylene. The GC yields were crotyl-DMM at 37%, α-methyl allyl-DMM at 20%, and bisalkylation at ~8%.

Reaction e6

To 50 ml of THF was added 0.10 ml (0.86 mmol) of Fe(CO)₂(NO)₂ and 2 ml @ 0.43M (0.86 mmol) of NaDMM in THF. After stirring for 3.2h one equivalent of NaDMM was added followed by a second equivalent an hour later. After another hour, a further 3 equivalents were added. The argon was displaced by introducing CO. The solution was stirred under static CO at room temperature for 14h then under bubbling CO at approximately -25°C for 4h. The solution mixture was allowed to

warm up to room temperature before adding 0.33g (1.5 mmol) of triphenyl phosphine (PPh₃). This solution was stirred under static CO for 72h followed by the addition of 0.59 ml (6.5 mmol) of 3-chloro-1-butene. The CO was displaced by argon and the solution mixture stirred for 24h before proceeding to the usual CF₃COOH, Et₂O / H₂O work-up. The mesitylene added was 0.4325g (3.6 mmol). The GC yields were α -methyl allyl-DMM at 13% and crotyl-DMM at 9%.

Reaction e7

To a solution of 20 ml of THF were added 1.6 mmol of Fe(CO)₂(NO)₂, 8.8 mmol (44 ml @ 0.20M) of NaDMM, 8.0 mmol of DMM, and 8.0 mmol (0.8 ml) of 3-chloro-1-butene. The solution was stirred at room temperature under a continuous argon flow. The reaction was monitored by IR. The solution mixture was worked-up by adding 8.8 mmol (0.77 ml) of CF₃COOH, extracting using Et₂O and H₂O, drying with MgSO₄, and adding mesitylene. The GC yields were α -methyl allyl-DMM at 72% and crotyl-DMM at 17%.

Reaction e8

Using the same reaction and work-up procedure as in reaction e7 and using the following quantities of reagents, GC yields of 14% for α -methyl allyl-DMM and 60% for crotyl-DMM were obtained: THF, 20 ml; NaDMM, 8.8 mmol (44 ml @ 0.20M); Fe(CO)₂(NO)₂, 1.6 mmol; crotyl chloride, 8.0 mmol (0.8 ml); and CF₃COOH, 8.0 mmol (0.7ml).

Reaction e9

To a 50 ml THF solution containing 0.81 mmol of NaDMM were added sequentially the following seven quantities of Fe(CO)₂(NO)₂: 0.1 eq (30 min.); 0.1 eq (30 min.); 0.1 eq (30 min.); 0.1 eq (20 min.); 0.1 eq (60 min.); 0.1 eq. (60 min.); and 0.2 eq (70 min). 1 eq was equal to 1 ml of a solution of 0.1 ml (0.86 mmol) of

$\text{Fe}(\text{CO})_2(\text{NO})_2$ dissolved in 10 ml of THF. After the final addition and stirring, the solvent was removed by vacuum evaporation leaving a dark brown-green residue. This was redissolved in 2.5 ml of THF and refluxed 2h. To the refluxing solution was added 0.1 ml (0.86 mmol) of 3-chloro-1-butene. 10 ml @ 0.42M (4.2 mmol) of NaDMM and a further 0.43 ml (4.2 mmol) of 3-chloro-1-butene. The solution was refluxed a further 2.5h. The solution was filtered over celite and the solvent was evaporated on a rotary evaporator. The residue was washed and extracted using a H_2O / Et_2O mixture and dried using MgSO_4 and filtered again. Mesitylene (0.606g, 5.04 mmol) was added and the GC yields were obtained: α -methyl allyl-DMM , 40%; crotyl-DMM , 24%; bisalkylation, ~8%.

3.6.3 The Allylic Acetates

α -methyl allyl acetate

Reaction e10

The NaDMM was prepared as previously described by adding 2.75 ml (24.2 mmol) of DMM in a Schlenk tube under argon to 75 ml of THF and 0.550g (11.8 mmol) of 50% oil dispersion NaH. This gave 11.5 mmol NaDMM and 12.7 mmol DMM. To this solution was added 0.12 ml (1.0 mmol) of $\text{Fe}(\text{CO})_2(\text{NO})_2$ and 1.29 ml (10.5 mmol) of α -methyl allyl acetate . The solution mixture was stirred 1h (the colour changing from red to green) and then refluxed for 3.5h. The work-up consisted of filtering over celite, evaporating the THF, redissolving in Et_2O , drying 15h with MgSO_4 , filtering and distilling at reduced pressure (95°C , ?mmHg). The isolated yield of α -methyl allyl-DMM (greater than 95% pure as assessed by GC) was 1.1g (5.9 mmol or 56%). The product was characterized by ^1H NMR.

Reaction e11 and e12

The same experimental and work-up procedure was used for both reactions e11 and e12. A 75 ml solution of THF with 11.9 mmol of NaDMM, 10.8 mmol of DMM, 1.1 mmol of $\text{Fe}(\text{CO})_2(\text{NO})_2$, and 10.8 mmol of crotyl acetate were refluxed for 3.5h. The solution was worked-up by filtering over celite, evaporating the THF, redissolving in Et_2O , drying with MgSO_4 , and filtering. After adding 0.166 mmol (1ml @ 0.166M) of mesitylene the GC yields were obtained. The GC yields for reaction e11 were, α -methyl allyl-DMM at ~3% (3.0 mmol), crotyl-DMM at 2% (0.17 mmol), and bisalkylation at 1%. The GC yields for reaction e12 were, α -methyl allyl-DMM at 32% (3.4 mmol), crotyl-DMM at ~2% (0.17 mmol), and bisalkylation at ~1%.

Reaction e13

A 75 ml solution of THF containing 1.1 mmol (0.13 ml) of $\text{Fe}(\text{CO})_2(\text{NO})_2$, 11.9 mmol of NaDMM, 10.8 mmol DMM and 10.8 mmol (1.3ml) of α -methyl allyl acetate was stirred at room temperature for 44h. The solution retained its dark red colour although a brown precipitate was formed. The THF solvent was removed by rotary evaporator and then the viscous residue was redissolved in Et_2O . A brown precipitate was formed. This was filtered over celite and the Et_2O evaporated yielding 0.925g of a pale yellow residue. The residue was taken up in 20 ml of anhydrous ether and 0.148g (1.23 mmol) of mesitylene added. The GC yields were α -methyl allyl-DMM at 15%, crotyl-DMM at <1%, and no bisalkylation.

Reaction e14

A solution of 75 ml of THF containing 11.9 mmol of NaDMM, 10.8 mmol of DMM and 10.8 mmol of α -methyl allyl acetate was refluxed for 25 minutes. This was followed by the addition of 1.1 mmol (0.13 ml) of $\text{Fe}(\text{CO})_2(\text{NO})_2$ and further refluxing for 9h. The solution mixture went from a dark red to brown with a tan precipitate. The work-up consisted of filtering the solution mixture over celite, evaporating the

THF, adding 0.161 g (1.34 mmol) of mesitylene, and redissolving in 50 ml of ether. The GC yields obtained were α -methyl allyl-DMM at 26%, crotyl-DMM at 1%, and bisalkylation at <1%.

Reaction e15

A 75 ml solution of THF containing 1.1 mmol (0.13 ml) of $\text{Fe}(\text{CO})_2(\text{NO})_2$, 11.9 mmol of NaDMM, 10.8 mmol of DMM and 10.8 mmol (1.34 ml) of α -methyl allyl acetate was prepared and refluxed for 2h. The solution was worked-up by filtering over celite, evaporating the solvent, taking up the residue in 50 ml of ether, drying over MgSO_4 and filtering. The amount of mesitylene added was 0.352g (2.9 mmol). The crude mixture yield was 1.431g and the GC product yields were α -methyl allyl-DMM at 38%, crotyl-DMM at <1%, and bisalkylation at <1%.

Reaction e16

To a 10 ml solution of THF containing 1.6 mmol (0.19 ml) of $\text{Fe}(\text{CO})_2(\text{NO})_2$ was added at room temperature 40 ml @ 0.20M (8.0 mmol) of NaDMM in THF, 0.91 ml (8.0 mmol) of DMM, and 1.0 ml (8.0 mmol) of α -methyl allyl acetate. After refluxing 6h, 0.62 ml (8.0 mmol) of CF_3COOH was added and the solvent evaporated using a rotary evaporator. The residue was redissolved in 100 ml of a 1:2 $\text{Et}_2\text{O}/\text{H}_2\text{O}$ mixture. The organic products were extracted into 3 x 50 ml Et_2O , dried 15h with MgSO_4 and filtered. 0.1086g (0.91 mmol) of mesitylene was added and the GC chromatograph was taken. The solvent was again removed by rotary evaporator and the product was isolated by column chromatography with a 10:1 hexane/ethyl acetate mixture as eluant. The GC yields were α -methyl allyl-DMM at 63%, crotyl-DMM at 4%, and bisalkylation at <1%. The isolated yields were α -methyl allyl-DMM at 0.88g (4.7 mmol) or 59% (greater than 95% pure as assessed by GC) and DMM at 0.19g (1.4 mmol) or 18%. Characterization was accomplished by ^1H NMR and GC.

crotyl acetate

Reaction e17

The NaDMM was prepared by adding 2.82 ml (24.8 mmol) of DMM, in a Schlenk tube under argon, to 75 ml of THF and 0.565g (11.8 mmol) of 50% oil dispersion NaH. This gave 11.8 mmol of NaDMM and 13.0 mmol of DMM. 0.12 ml (1.0 mmol) of $\text{Fe}(\text{CO})_2(\text{NO})_2$ and 1.33 ml (10.7 mmol) of crotyl acetate were added to this solution. The solution was stirred 1h whereupon it changed from a red to a green colour, and then refluxed for 3.5h. The work-up consisted of filtering over celite, evaporating the THF, redissolving in Et_2O , drying 15h with MgSO_4 , filtering and distilling at reduced pressure (116°C , ?mmHg). The isolated yield of crotyl-DMM (greater than 95% pure as assessed by GC) was 1.1g (5.9 mmol) or 55%. The product was characterized by ^1H NMR.

Reaction e18 and e19

Using the same experimental and work-up procedure for both reactions e18 and e19, two reaction flasks, each containing a 75 ml solution of THF with 11.9 mmol of NaDMM, 10.8 mmol of DMM, 1.1 mmol of $\text{Fe}(\text{CO})_2(\text{NO})_2$ and 10.8 mmol of crotyl acetate, were refluxed for 3.5h. They were then worked-up by filtering over celite, evaporating the THF, redissolving in Et_2O , drying with MgSO_4 , filtering, and after adding 0.166 mmol (1ml @ 0.166M) of mesitylene analyzed by GC. The GC yields for reaction e18 were α -methyl allyl-DMM at 3%, crotyl-DMM at 53%, and bisalkylation at 2%. The GC yields for reaction e19 were α -methyl allyl-DMM at ~1%, crotyl-DMM at 49%, and bisalkylation at 2%.

Reaction e20

To 20 ml of THF was added, at room temperature, 10 ml (0.84 mmol) of $\text{Fe}(\text{CO})_2(\text{NO})_2$, 50 ml @ 0.17M (8.5 mmol) of NaDMM in THF, 0.98 ml (8.6 mmol)

of DMM and 1.0 ml (8.0 mmol) of crotyl acetate . This solution was refluxed for 2h followed by the evaporation of the THF and extraction of the residue with 100 ml of NH_4^+Cl^- and 4 x 50 ml of CH_2Cl_2 . It was then dried with MgSO_4 and 0.160g (1.30 mmol) of mesitylene was added. The GC yields were α -methyl allyl-DMM at 1.4%, crotyl-DMM at 52%, and bisalkylation at ~2%.

Reaction e21

To 20 ml THF were added 1.0 ml (0.84 mmol) of $\text{Fe}(\text{CO})_2(\text{NO})_2$, 50 ml @ 0.17M (8.5 mmol) of NaDMM in THF and 0.98 ml (8.6 mmol) of DMM. This solution was refluxed for 2h followed by the addition of 1.0 ml (8.0 mmol) of crotyl acetate . This was refluxed for another 2h. The work-up proceeded as usual but with a CH_2Cl_2 / 1% aqueous HCl solution for the extraction. Mesitylene (0.11g, 0.92 mmol) was added and the following GC yields were obtained: α -methyl allyl-DMM , 0.4%; crotyl-DMM , 12%.

Reaction e22

To 20 ml of THF were added at room temperature 1.0 ml (0.84 mmol) of $\text{Fe}(\text{CO})_2(\text{NO})_2$, 50 ml @ 0.17M (8.5 mmol) of NaDMM in THF, 0.91 ml (8.0 mmol) of DMM, and 1.0 ml (8.0 mmol) of crotyl acetate . The reaction was refluxed 2h. The work-up was performed as usual with CH_2Cl_2 /1% aqueous HCl as the extraction solvents and the addition of 0.153g (1.30 mmol) of mesitylene. The GC yields were α -methyl allyl-DMM at 2%, crotyl-DMM at 62%, and bisalkylation at ~2%.

Reaction e23

To a solution of THF containing 0.19 ml (1.6 mmol) of $\text{Fe}(\text{CO})_2(\text{NO})_2$ was added at room temperature 40 ml 0.20M (8.0 mmol) of NaDMM in THF, 0.91 ml (8.0 mmol) of DMM, and 1.0 ml (8.0 mmol) of crotyl acetate . After refluxing 6h, 0.62 ml (8.0 mmol) of CF_3COOH was added and the solvent was evaporated using a rotary

evaporator. The residue was redissolved in 100 ml of a 1:2 Et₂O/H₂O mixture. The organic products were extracted into 3 x 50 ml Et₂O, dried 15h with MgSO₄ and filtered. 0.111g (0.93 mmol) of mesitylene was added and the GC chromatograph was obtained. The solvent was again removed by rotary evaporator and the product was isolated by column chromatography with a 10:1 hexane/ethylacetate mixture as eluant. The GC yields were α -methyl allyl-DMM at 8%, crotyl-DMM at 61%, and bisalkylation at <5%. The isolated yields were crotyl-DMM at 50% (0.75g, 4.0 mmol) and DMM at 25% (0.26g, 2.0 mmol). Characterization was accomplished by ¹H NMR and GC.

Reaction e24

CO gas was bubbled through a 30 ml solution of THF containing 0.8 mmol (1ml @ 0.8M) of Fe(CO)₂(NO)₂ and 8.0 mmol (4.0 ml @ 0.2M) of NaDMM for a period of 1h. This was followed by the addition of 0.91 ml (8.0 mmol) of DMM and 1.0 ml (8.0 mmol) of crotyl acetate . The reaction was monitored by IR. The solution, which was green, was heated in an oil bath at 50°C for 9h under a continuous flow of CO. Some of the solvent evaporated. The solution remained green although a residue formed along the sides of the flask. 40 ml of THF was added and the solution reheated to 50°C for 1h. The solution was heterogeneous and a tan colour. The heating was stopped and the solution was left under static CO for 24h. The usual work-up gave GC yields (mesitylene; 0.50 ml, 0.36 mmol) of: α -methyl allyl-DMM , 6%; crotyl-DMM , 54%; and bisalkylation, <5

Phenyl Allyl Acetates

Reaction e25

To a solution containing 0.5 mmol (10 ml @ 0.05M) of Fe(CO)₂(NO)₂, 2.5 mmol

(28 ml @ 0.1M) of NaDMM in THF and 2.5 mmol (0.33g) of DMM was added 2.5 mmol (0.44g) of cinamyl acetate . The solution was brought to reflux and monitored by IR for 16h followed by the addition of CF₃COOH. The work-up consisted of evaporation of the THF and extraction using Et₂O and H₂O. The organic phase was dried with MgSO₄ followed by the evaporation of the Et₂O. The products were separated by column chromatography using a 10:1 hexane, ethyl acetate mixture as eluant. The yield was 0.038g (1.24 mmol or 50%) of cinamyl-DMM with no appreciable amounts of α -phenyl allyl-DMM . This was verified by GC and the product characterized by ¹H NMR and GC-MS.

Reaction e26

Using the same experimental, work-up and isolation procedure as in reaction e25, 0.5 mmol of Fe(CO)₂(NO)₂, 2.8 mmol of NaDMM, 2.5 mmol of DMM and 2.5 mmol of α -phenyl allyl acetate yielded 0.146g (0.589 mmol or 24%) of α -methyl allyl-DMM and 0.064g (0.26 mmol or 10%) of cinamyl-DMM . This was verified by GC and the products characterized by ¹H NMR and GC-MS.

geranyl acetate

Reaction e27

To a 50 ml solution of THF containing 1.0 mmol (0.12 ml) of Fe(CO)₂(NO)₂ and 3.5 mmol (33 ml @ 0.1M) of NaDMM was added 0.644g (3.3 mmol) of geranyl-acetate. The solution was refluxed for 24h. It was worked-up by adding CF₃COOH, evaporating the solvent, extracting with Et₂O and H₂O, drying with MgSO₄, and then adding 0.0725g (0.604mmol) of mesitylene. The GC yield was 25% in alkylated product with a 2.5:1 ratio of geranyl-DMM to neryl-DMM . More than 40% of the geranyl acetate was unreacted as shown by GC. The products were characterized by

<i>Rx time</i>	<i>GOAc</i>	<i>GDMM</i>
0:30	1.02	0
1:45	0.93	0
3:40	0.98	0.13
7:00	1.09	0.22
17:00	0.63	0.42
21:30	0.57	0.62
24:00	0.35	0.49
30:10	0.40	0.88

Table 3.5: Values for the plot of the disappearance of starting material and appearance of products over time for reaction e29.

¹H NMR.

Reaction e28

To 20 ml of THF were added sequentially 0.87 mmol (0.149g) of $\text{Fe}(\text{CO})_2(\text{NO})_2$, 2.9 mmol (29 ml @ 0.10 M) of NaDMM and 2.62 mmol (0.5144g) of geranyl acetate. This solution was stirred at room temperature for 42h and monitored by IR. It was then refluxed for 24h. CF_3COOH was added to the solution and the solvent was evaporated. The residue was extracted with Et_2O and H_2O , dried with MgSO_4 , and mesitylene (0.090g, 0.75 mmol) added. The GC yield in alkylated product was 32% with a geranyl-DMM /neryl-DMM ratio of 3.2:1. The GC also showed that more than 40% of the geranyl acetate was unreacted.

3.7 The $\text{Fe}(\text{CO})_3(\text{NO})^-$ Alkylation Reactions With Geranyl Acetate

3.7.1 $\text{Fe}(\text{CO})_3(\text{NO})^- \text{Na}^+ \cdot \text{MeOH}$

Reaction e29

To 0.1968g (0.87 mmol) of $\text{Fe}(\text{CO})_3(\text{NO})^- \text{Na}^+ \cdot \text{CH}_3\text{OH}$ in 45 ml of THF were added 19.0 @ 0.1M of NaDMM, 0.341g (1.74 mmol) of geranyl acetate, and 0.165g

(1.38 mmol) of mesitylene. The solution mixture was brought to reflux and over a period of 4.4h, 10 aliquots of 1 ml each were obtained by syringe from the refluxing mixture, filtered over celite and cotton plug in a Pasteur pipette and analyzed by IR and GC. With the GC traces, a plot of the disappearance of starting material and appearance of products over time was obtained.

Reaction e30

A solution containing 30 ml of THF, 12 ml @ 0.10M of NaDMM, and 0.2225g (1.14 mmol) of geranyl acetate were refluxed for 48h. The solution remained colourless and clear with some milky precipitate. The reaction mixture was worked-up by adding CF_3COOH , evaporating the solvent, extracting with Et_2O and H_2O , drying with MgSO_4 , filtering, and then adding 0.0518g (0.432 mmol) of mesitylene. GC analysis showed there was approximately 10% geranyl-DMM formed.

Reaction e31

To a 30 ml solution of THF containing 0.344g (1.53 mmol) of $\text{Fe}(\text{CO})_3(\text{NO})^- \text{Na}^+$ CH_3OH was added 30.6 ml @ 0.10M (3.06 mmol) of NaDMM, 0.4036g (3.06 mmol) of DMM and 0.545g (2.78 mmol) of geranyl acetate. The reaction was brought to reflux and the disappearance of the NaDMM was monitored by withdrawal of an aliquot of the solution and analysis of it by IR. After 42h, with no NaDMM peak (1650 cm^{-1}) present in the IR, 2 ml of CF_3COOH were added and the solvent evaporated by rotary evaporator. The residue was then taken up in 50 ml of CH_2Cl_2 and 0.080g (6.7 mmol) of mesitylene. GC analysis gave an alkylated products yield of 54% with a geranyl-DMM/neryl-DMM ratio of 3.1:1. Isolation by preparative TLC gave 0.348 g (1.30 mmol) or 47% of a geranyl-DMM /neryl-DMM mixture.

Reaction e32

To 15 ml of THF were added 0.1568g (0.697 mmol) of $\text{Fe}(\text{CO})_3(\text{NO})^- \text{Na}^+$.

CH₃OH, 15.3 ml @ 0.1M of NaDMM, 0.183g (1.39 mmol) of DMM, and 0.276 g (1.41 mmol) of geranyl acetate . The solution mixture was refluxed 43h then worked-up in the usual manner with CF₃COOH, Et₂O and H₂O. Mesitylene was added (0.1085g, 0.904 mmol) and the GC yield in geranyl-DMM /neryl-DMM product was 1.07 mmol (76%) with a geranyl-DMM /neryl-DMM ratio of 3.2:1. There was no unreacted geranyl acetate.

Reaction e33

To 15 ml of THF were added 0.104 g (0.462 mmol) of Fe(CO)₃(NO)⁻Na⁺ - CH₃OH, 16.9 ml @ 0.1M of NaDMM, 0.203g (1.54 mmol) of DMM, and 0.302g (1.54 mmol) of geranyl acetate . The solution was refluxed for 43h followed by the addition of 30 ml of THF because of partial evaporation of the solvent. The reaction was refluxed a further 5h before being worked-up in the usual manner with CF₃COOH, Et₂O and H₂O. Mesitylene was added (0.0878g, 0.732 mmol) and the GC yield in geranyl-DMM /neryl-DMM product was 0.95 mmol (62%) with a geranyl-DMM /neryl-DMM ratio of 3.7:1. There was less than 15% of unreacted geranyl acetate .

Reaction e34

To 40 ml of THF were added 0.1935g (0.86 mmol) of Fe(CO)₃(NO)⁻Na⁺-CH₃OH, 17.2 ml @ 0.1M (1.72 mmol) of NaDMM, 0.196 ml (1.72 mmol) of DMM, 0.3346g (1.7 mmol) of geranyl acetate , and 0.035 ml (0.86 mmol)of CH₃OH. The solution mixture was refluxed 42h followed by the addition of 0.3 ml of CF₃COOH. The solution was worked-up by the usual Et₂O/H₂O extraction and with 0.089g (0.074 mmol) of mesitylene being used as the GC internal standard. The GC yield was 1.1 mmol of geranyl-DMM/neryl-DMM or 65% with a geranyl-DMM /neryl-DMM ratio of 2.3:1. There was less than 15% unreacted geranyl acetate .

3.7.2 $\text{Fe}(\text{CO})_3(\text{NO})^- \text{Na}^+$ In Situ

Reaction e35 and e36

Under continuous argon flow, 0.497g (1.44 mmol) of $\text{Fe}(\text{CO})_4^2-2\text{Na}^+-1.5$ dioxane was transferred from a storage schlenk to the reaction vessel schlenk e35. To this were added 60 ml of THF and 0.217g (1.27 mmol) of $\text{Fe}(\text{CO})_2(\text{NO})_2$, thus resulting in 2.54 mmol of $\text{Fe}(\text{CO})_3(\text{NO})^- \text{Na}^+$. 40 ml of this solution was transferred by syringe to a second schlenk e36. To schlenk e35 was added 0.335g (2.54 mmol) of DMM. To each schlenk, e35 and e36, were added 25.4 ml @ 0.1M (2.54 mmol) of NaDMM and 0.498g (2.54 mmol) of geranyl acetate. The solution mixtures were refluxed 45h. Both reactions were worked-up by adding CF_3COOH , evaporating the solvent, extracting with $\text{CH}_2\text{Cl}_2/2\%$ aqueous HCl, drying with MgSO_4 , and re-evaporating the solvent. The products from schlenk e35 were isolated by column chromatography using a 10:1 hexane / ethylacetate mixture whereas the products from schlenk e36 were isolated by preparative TLC with a first elution using pure hexane and a second elution using a 20:1 hexane/ ethyl acetate mixture. The isolated alkylated products yields were 50% or 0.3118g (1.16 mmol) for e35 with a geranyl-DMM /neryl-DMM ratio of 3.0:1 and 54% or 0.3379g (1.76 mmol) for e36 with a ratio of 3.1:1.

3.7.3 $\text{Fe}(\text{CO})_3(\text{NO})^- \text{Na}^+ \cdot 1,4\text{-dioxane}$

Reaction e37

To 0.129g (0.46 mmol) of $\text{Fe}(\text{CO})_3(\text{NO})^- \text{Na}^+ \cdot 1,4$ dioxane were added 20 ml of THF 23.1 ml @ 0.10M of NaDMM, 0.24ml (2.10 mmol) of DMM, and 0.412g (2.10 mmol) of geranyl acetate. The reaction mixture was refluxed for 45h and monitored by IR. After adding CF_3COOH and working-up in the usual manner, 0.0877g of mesitylene was added. The GC yield in geranyl-DMM /neryl-DMM product mixture

was 1.5 mmol or 71% with a ratio of 3.0:1. GC showed no unreacted geranyl acetate . Preparative TLC product yield was 52% or 0.290g (1.1 mmol).

Reaction e38

To a solution of 25 ml @ 0.10M of NaDMM in THF were added 0.332g (1.18 mmol) of $\text{Fe}(\text{CO})_3(\text{NO})^- \text{Na}^+$ 1,4 dioxane and 0.444g (2.27 mmol) of geranyl acetate . The solution was refluxed and monitored by IR for a period of 46.5h then worked-up in the usual manner with CF_3COOH , Et_2O and H_2O . Mesitylene was added (0.120g, 0.100 mmol) and the obtained GC yield was 69% of geranyl-DMM and neryl-DMM . There was no unreacted geranyl acetate . The amount of product isolated by column chromatography was 0.268g (1.0 mmol) or 44%. The isolated product was characterized by ^1H NMR.

Reaction e39

To a solution of 60 ml @ 0.10 M of NaDMM in THF was added 0.478g (1.70 mmol) of $\text{Fe}(\text{CO})_3(\text{NO})^- \text{Na}^+$ 1,4 dioxane. 30 ml of this solution was transferred by syringe to a second schlenk and used in reaction e46. To the remaining 30 ml, now containing 0.85 mmol of $\text{Fe}(\text{CO})_3(\text{NO})^- \text{Na}^+$ 1,4-dioxane , was added 0.5284g (2.69 mmol) of geranyl acetate. The solution refluxed for 46.5h. The solution was then worked-up in the usual manner with CF_3COOH , Et_2O and H_2O , and addition of 0.123g (1.03 mmol) of mesitylene. The GC yield in geranyl-DMM /neryl-DMM product mixture was 60%. There was very little unreacted geranyl acetate .

Reaction e40

To the 30 ml @ 0.10 M (3.0 mmol) of NaDMM and 0.027M (0.85 mmol) of $\text{Fe}(\text{CO})_3(\text{NO})^- \text{Na}^+$ -1,4 dioxane in THF, as prepared in reaction e40, were added a further 30 ml @ 0.10M of NaDMM in THF and 1.048g (5.34 mmol) of geranyl acetate . The solution was refluxed for 46.5h then worked-up in the usual manner

<i>Rx time</i>	<i>GOAc</i>	<i>GDMM</i>
0:30	1.02	0
1:45	0.93	0
3:40	0.98	0.13
7:00	1.09	0.22
17:00	0.63	0.42
21:30	0.57	0.62
24:00	0.35	0.49
30:10	0:40	0.88

Table 3.6: Values for the plot of the disappearance of starting material and appearance of products over time for reaction e41.

with CF_3COOH , Et_2O , and H_2O . Adding 0.116g (0.97 mmol) of mesitylene the GC yield obtained in geranyl-DMM / neryl-DMM product mixture was 51%. There was >20% of unreacted geranyl acetate .

3.8 $\text{Fe}(\text{CO})_3(\text{NO})^- \text{Na}^+$, Allyl Acetate Reaction

Reaction e41

To 30 ml of THF were added 0.0984g (0.44 mmol) of $\text{Fe}(\text{CO})_3(\text{NO})^- \text{Na}^+ \cdot \text{CH}_3\text{OH}$, 0.176g (0.176 mmol) of allyl acetate, 0.153g (1.27 mmol) of mesitylene, and 17.6 ml @ 0.10M of NaDMM. The solution was refluxed for 30.5h During this time 8x1 ml aliquots of the solution were filtered over celite and a cotton plug in a Pasteur pipette and analyzed by GC. The decrease in starting material and the increase in product were plotted over time. In the first 18h the solution was yellow. Between 18 and 22h the solution turned dark brown. No NaDMM remained in the IR.

3.9 Reactions with $\text{Fe}(\text{CO})_2(\text{NO})_2$, $\text{Fe}(\text{CO})_3(\text{NO})^- \text{Na}^+$, and Geranyl Acetate

Reaction e42

To 40 ml of THF were added 0.0772g (0.449 mmol) of $\text{Fe}(\text{CO})_2(\text{NO})_2$, 0.296g (2.25 mmol) of DMM, and 0.430g (2.24 mmol) of geranyl acetate . As soon as this solution was brought to reflux, NaDMM (24.6 ml @ 0.1M, 2.46 mmol) was added dropwise over a period of 50 minutes. The refluxing was continued for 48h then stopped. The solution was stirred at room temperature, under argon flow for 5 days. After which 15 ml of THF and 0.118g (0.52mmol) of $\text{Fe}(\text{CO})_3\text{NO}^-$ were added. The new solution was refluxed 42h then quenched with 0.35 ml of CF_3COOH . The solution was worked-up using Et_2O and H_2O extractions. The GC yield, after having added 0.0812g (0.677 mmol) of mesitylene was 0.94 mmol or 43% in geranyl-DMM /neryl-DMM product with a 2.1:1 ratio. There was much unreacted geranyl acetate (>50%) as indicated by GC. A GC of the solution mixture prior to the addition of $\text{Fe}(\text{CO})_3(\text{NO})^-$ indicated that there was no product formation with the $\text{Fe}(\text{CO})_2(\text{NO})_2$.

Reaction e43

To 0.147g (0.65 mmol) of $\text{Fe}(\text{CO})_3(\text{NO})^- \text{Na}^+ - \text{CH}_3\text{OH}$ were added 20 ml of THF, 0.124g (0.72 mmol) of $\text{Fe}(\text{CO})_2(\text{NO})_2$, 50.3 ml @ 0.10M of NaDMM, 0.52 ml (4.57 mmol) of DMM, and 0.896g (4.57 mmol) of geranyl acetate . The reaction mixture was refluxed 41h. IR monitoring showed that there was unreacted NaDMM. The reaction was quenched with CF_3COOH and worked-up in the usual manner with Et_2O and H_2O . Addition of 0.1085g (0.904 mmol) of mesitylene followed by GC analysis indicated a yield in geranyl-DMM /neryl-DMM of 2.8 mmol or 42% with a ratio of 3.7:1 respectively. There was 30% of unreacted geranyl acetate .

Bibliography

- [1] B.M. Trost, T.R. Vorhoeven, *Comprehensive Organometallic Chemistry*; Pergamon: Oxford, 1982; Vol. 8, pp 799-938
- [2] J. Tsuji, *J. Organomet. Chem.*, 1986, 300, 281
- [3] B.M. Trost, *Acc. Chem. Res.*, 1980, 12, 198
- [4] B.M. Trost, *Pure & Appl. Chem.*, 1981, 53, 2357
- [5] B.M. Trost, *Chem. in Brit.*, 1984, 20(4), 315
- [6] B.M. Trost, Ming-Hong Hung, *J. Am. Chem. Soc.*, 1983, 105, 7757
- [7] T. Cuvigny, M. Julia, *J. Organomet. Chem.*, 1983, 250, C21
- [8] B.L. Buckwalter, *J. Am. Chem. Soc.*, 1978, 100, 6445
- [9] I. Minami, I. Shimizu, J. Tsuji, *J. Organomet. Chem.*, 1985, 296
- [10] S. Suzuki, M. Shiano, Y. Fugita, *Synthesis*, 1983, 804
- [11] I.T. Harrison, E. Kimurd, E. Bohme, J.H. Fried, *Tetrahedron Lett.*, 1969, 1589
- [12] B.M. Trost, P. Metzuer, *J. Am. Chem. Soc.*, 1980, 102, 3572
- [13] I. J. Harvie, F.J. McQuillin, *J. Chem. Soc., Chem. Comm.*, 1978, 747
- [14] B.M. Trost, *Tetrahedron*, 1977, 33, 2615

- [15] B.M. Trost, L. Weber, P.E. Strege, T.S. Fulluton, T.J. Dietsche, *J. Am. Chem. Soc.*, 1978, 100, 3426
- [16] M. Oslinger, S. Powell, *Can. J. Chem.*, 1973, 96, 274
- [17] T. Cuvigny, M. Julia, C. Rolando, *J. Organomet. Chem.*, 1985, 285, 395
- [18] L.S. Hegedus, T. Hayashi, W.H. Darlington, *J. Am. Chem. Soc.*, 1978, 100, 7747
- [19] B.M. Trost, N.R. Schumff, *J. Am. Chem. Soc.*, 1985, 107, 396
- [20] J. Tsuji, I. Shimizu, I. Minami, *Tetrahedron Lett.*, 1983, 24, 50, 5635
- [21] J. Tsuji, I. Shimizu, I. Minami, *Tetrahedron Lett.*, 1983, 24, 50, 5639
- [22] J. Tsuji, I. Shimizu, I. Minami, *Tetrahedron Lett.*, 1983, 24, 43, 4713
- [23] B.M. Trost, J.W. Herndur, *J. Am. Chem. Soc.*, 1984, 106, 6835
- [24] B.M. Trost, T.P. Klum, *J. Am. Chem. Soc.*, 1979, 101, 6756
- [25] B.M. Trost, P.E. Strege, *J. Am. Chem. Soc.*, 1977, 99, 1649
- [26] B.M. Trost, Ming-Hong Hung, *J. Am. Chem. Soc.*, 1984, 106, 6837
- [27] B.M. Trost, M. Lautens, *J. Am. Chem. Soc.*, 1982, 104, 5543
- [28] B.M. Trost, M. Lautens, *J. Am. Chem. Soc.*, 1983, 105, 3343
- [29] L.S. Hegedus, Yoshio Inove, *J. Am. Chem. Soc.*, 1982, 104, 4917
- [30] J.-L. Roustan, J.Y. Merour, F. Houlihan, *Tetrahedron Lett.*, 1979, 39, 3721
- [31] G.S. Silverman, S. Strickland, K.M. Nicholas, *Organometallics*, 1986, 5, 2117

- [32] Yuanyao Xu, Bo Zhou, *J. Org. Chem.*, 1987, 52, 974
- [33] J.L. Roustan, A. Forgues, J.Y. Merour, N.D. Venayak, B. Morrow, *Can. J. Chem.*, 1983, 61, 1339
- [34] R.B. King, *Organometallic Synthesis*, Vol. 1, p. 167. Academic Press, New-York, 1965.
- [35] W. Hiebner, H. Beutner, *Z. Anorg. Allg. Chem.*, 1963. 320, 285
- [36] M. Cygler, F.R. Ahmed, A. Forgues, J.-L. Roustan, *Inorg. Chem.*, 1983, 22, 1026
- [37] K.H. Pannel, Sen Chen Yu, K.L. Belknap, *J. Chem. Soc., Chem. Comm.*, 1977, 362
- [38] H.J. Kurosawa, *J. Chem. Soc. Dalton*, 1979, 939
- [39] J.L. Roustan, M. Bisnaire, G. Park, P. Guillaume, *J. Organomet. Chem.*, 1988, 356, 195
- [40] S.A. Godleski, K.B. Gundlach, H.Y. Ho, E. Keinan, F. Frolow, *Organometallics*, 1984, 3, 21
- [41] K.H. Pannell, Y.S. Chen, K. Belknap, C.C. Wu, I. Bernal, M.W. Creswick, H.N. Huang, *Inorg. Chem.*, 1983, 22, 418
- [42] J.L. Roustan, N.D. Venayak, F. Houlihan, unpublished results